Bayesian Passive Sonar Tracking in the Context of Active-Passive Data Fusion

by

Bryan Alan Yocom, B.S.

THESIS

Presented to the Faculty of the Graduate School of

The University of Texas at Austin

in Partial Fulfillment

of the Requirements

for the Degree of

MASTER OF SCIENCE IN ENGINEERING

THE UNIVERSITY OF TEXAS AT AUSTIN

August 2009

Bayesian Passive Sonar Tracking in the Context of Active-Passive Data Fusion

APPROVED BY

SUPERVISING COMMITTEE:

Mark F. Hamilton, Supervisor

Brian R. La Cour

Thomas W. Yudichak

To my parents, Rayburn and Sandra Yocom.

Acknowledgments

I would first like to thank my parents for their constant support through my college career and beyond. Without them I'm not sure this work would have been possible. I also owe many thanks to my research advisers Brian La Cour and Tom Yudichak for being sincere friends and mentors. Their help, knowledge, and advice was invaluable. Brian, in particular, served me well as a veritable encyclopedia for all things mathematics, statistics, or LaTeX related. Jason Aughenbaugh has also been a valuable source of information and good conversation during my time at ARL. Thanks also go to Mark Hamilton for being an excellent academic adviser and a constant source of encouragement and advice.

Thanks are also due to many of the great course instructors I had at UT for their support and advice. This includes Hao Ling, Mark Hamilton, Brian Evans, David Blackstock, Michael Haberman, Preston Wilson, and Neal Hall. I hope to put all of your knowledge to good work. Data from the SEABAR 07 seatrial was provided by the NATO Undersea Research Centre (NURC), in collaboration with the U.S. Office of Naval Research (ONR). Finally, I would like to thank Applied Research Laboratories as well as Keith Davidson and John Tague from the Office of Naval Research for supporting this work.[1]

[1]This work was supported by the Office of Naval Research under contract no. N00014-06-G-0218-01.

Bayesian Passive Sonar Tracking in the Context of Active-Passive Data Fusion

Bryan Alan Yocom, M.S.E.
The University of Texas at Austin, 2009

Supervisor: Mark F. Hamilton

This thesis investigates the improvements that can be made to Bayesian passive sonar tracking in the context of active-passive sonar data fusion. Performance improvements are achieved by exploiting the prior information available within a typical Bayesian data fusion framework. The algorithms developed are tested against both simulated data and data measured during the SEABAR 07 sea trial. Results show that the proposed approaches achieve improved detection, decreased estimation error, and the ability to track quiet targets in the presence of loud interferers.

Table of Contents

Acknowledgments **v**

Abstract **vi**

List of Tables **ix**

List of Figures **x**

Chapter 1. Introduction **1**

Chapter 2. Background **4**

2.1 Model 4

2.1.1 Physical Model 4

2.1.2 Data Model 5

2.1.3 Statistical Model 8

2.2 Beamforming 10

2.2.1 Conventional Beamforming 11

2.2.2 Optimum Beamforming 13

2.2.2.1 Minimum Variance Distortionless Response 13

2.2.2.2 Minimum Power Distortionless Response 14

2.2.3 Adaptive Beamforming 15

2.2.4 Robust Adaptive Beamforming 15

2.2.5 Beamforming Example 17

2.3 Prior Information 20

2.4 Bayesian Tracking 21

Chapter 3. The Single-Signal Likelihood Function **24**

3.1 Statistical Model 24

3.2 Single-Signal Likelihood Function in the Absence of Interferers 27

3.3 Single-Signal Likelihood Function in the Presence of Interferers 28

3.4 Marginalization of the Joint Likelihood Function 32

3.4.1 Probabilistic Approach 32

3.4.2 Currently Implemented Approximations 35
3.4.3 Proposed Approach 36
3.4.3.1 Maximum Likelihood Estimation 36
3.4.3.2 Signal and Noise Power Maximum Likelihood Estimates 37
3.4.3.3 Alternating Maximization Algorithm 39

Chapter 4. Utilization of Prior Information 41
4.1 TOI in the Presence of a Known Number of Interferers 41
4.1.1 Introduction 41
4.1.2 Cued Beamforming 42
4.1.3 Feedback of Maximum Likelihood Estimates 45
4.1.4 Proposed Approach 47
4.1.5 Performance Analysis 49
4.2 TOI in the Presence of an Unknown Number of Interferers 53
4.2.1 Introduction 53
4.2.2 Data Association 54
4.2.2.1 Discussion 54
4.2.2.2 Association Probabilities 55
4.2.2.3 Association Techniques 59
4.2.3 Proposed Approach 60
4.2.4 Performance Analysis 63
4.2.4.1 Description and Preliminary Analysis of SEABAR 07 Sea Trial 63
4.2.4.2 Adding Robustness to the Signal Processing 70
4.2.4.3 Results 72

Chapter 5. Conclusions and Future Work 78

Appendix A. Approximation of the Association Likelihood Function 80

Bibliography 82

Vita 89

List of Tables

3.1 Alternating maximization (AM) algorithm – conventional approach. . 40

4.1 Alternating maximization (AM) algorithm – proposed approach with known number of interferers. 48

4.2 Alternating maximization (AM) algorithm – proposed approach with unknown number of interferers. 61

4.3 Total algorithm for computing the single-signal likelihood function – proposed approach with unknown number of interferers. 63

4.4 Names of vessels reported by AIS and assigned numbers. 64

List of Figures

2.1 An example target and sensor model. 4

2.2 A general narrowband beamformer implemented in the frequency domain. 12

2.3 A delay-and-sum beamformer implemented in the time domain. . . . 12

2.4 Beampatterns for various beamformers. The dotted lines represent the SOI at 80° and two interferers at 40° and 150°. 18

2.5 Beamformer output power for various beamformers. The dotted lines represent the SOI at 80° and two interferers at 40° and 150°. 19

3.1 Various terms of the single-signal log-likelihood function. The dotted lines represent the SOI at 80° and two interferers at 40° and 150°. . . 29

3.2 The single-signal log-likelihood function. The dotted lines represent the SOI at 80° and two interferers at 40° and 150°. The dashed line represents the no-signal log-likelihood. 30

3.3 Single-signal log-likelihood function marginalized through direct integration. Interferer prior PDFs are insufficiently localized. The dotted lines represent the SOI at 80° and two interferers at 40° and 150°. The dashed line represents the no-signal log-likelihood. 33

3.4 Single-signal log-likelihood function marginalized through direct integration. Interferer prior PDFs are sufficiently localized. The dotted lines represent the SOI at 80° and two interferers at 40° and 150°. The dashed line represents the no-signal log-likelihood. 34

4.1 An example of the cued beam algorithm. (a) shows the prior PDF in bearing, and (b) shows the prior PDF in u-space. The prior CDF and the inverse of the prior CDF are shown in (c) and (d), respectively. The dotted lines in (d) show the values of u for $J = 20$ generated MRAs. 46

4.2 Cued Beam MRAs for the prior PDF in Figure 4.1(a). 47

4.3 Performance of moving target without interferers. The solid lines represent the proposed approach and the dashed lines the conventional alternating maximization (AM) approach. 51

4.4 Performance of moving target with interferers. The solid lines represent the proposed approach and the dashed lines the conventional alternating maximization (AM) approach. 52

4.5 SEABAR 07 AIS Tracks for run A01. The Leonardo (the TOI) is in red and the Alliance (pulling the Atlas array) is in black. Blue tracks represent potential interferers. See the legend in Table 4.4 to find the names of the numbered interferers. 62

4.6 BTR showing AIS position information. The Leonardo is shown in red and labeled 0. The tracks for potential interferers are shown in varying colors. See the legend in Table 4.4 to find the names of the numbered interferers. 65

4.7 Posterior log-PDF for the Leonardo at a time of 106 minutes with targets 1-10 modeled as interferers, ML estimates used for signal powers, and MAP data association performed. The current position of the targets and receivers are shown by circles. Dotted and solid lines show the past trajectories. Notice the sharp maneuvers made by the Leonardo. 67

4.8 BTR showing adaptive beamformer output power. The beamformer used here is a simple, unconstrained minimum power distortionless response (MPDR) filter [48]. 68

4.9 SPED ED BTR for 800-1100Hz frequency band [14]. The beamformer output power shown in Figure 4.8 was used as the input to the SPED processing. 69

4.10 Estimated BTRs, results for underestimated model order. 74

4.11 Estimated BTRs, results for various model orders. 76

Chapter 1

Introduction

Data fusion has become an increasingly popular topic in a number of fields [24]. One of its main goals is the collection of information gathered from multiple sources to increase the accuracy of signal detection, parameter estimation, and target tracking. Additionally, authors have suspected for some time that the integration of active and passive sonar systems should improve performance because of the complementary information the two systems provide [44]. Specifically, active sensors give a good estimate of range and bearing, while passive sensors are most efficient at estimating the bearing and radiated spectrum of a target. It is therefore natural to apply data fusion to active and passive sonar systems.

A data fusion framework provides a unique opportunity to utilize prior information. Previous work has explored the use of prior information in active sonar systems [2]. The work in this thesis is focused on exploiting available prior information to improve the signal processing of a passive sonar horizontal line array (HLA). More specifically, it explores the problem of passive detection and tracking of a single target of interest (TOI) in the presence of ambient background noise. Additional targets may also be present that emit loud signals that interfere with the detection and estimation of the TOI.

The use of passive sonar for target tracking is a well studied problem. Oftentimes tracking filters make many simplifying assumptions. Typically, it is assumed

that the target's position and velocity have a Gaussian distribution, the observed data follow linear relations (i.e. measurements have a linear mapping to target state), and that measurement errors are Gaussian. The resulting solution is the well known Kalman filter tracker [25]. Although Kalman filtering can sometimes lead to simple, effective solutions, its application is limited to specific, well-behaved scenarios. When its assumptions are violated efforts are made to linearize measurements about the current mean state estimate [4]. Although such approaches can provide reasonable results in many scenarios, Bayesian filtering provides a more rigorous solution.

The Kalman filter is, in fact, simply a special case of the more general Bayesian filter [45]. Bayesian filtering inherently allows for non-linearity in observations as well as non-Gaussian target dynamics and measurement errors. When the assumptions of the Kalman filter are met, the Bayesian filter and Kalman filter solutions converge to the same answer. In the case of passive sonar, Bayesian filtering is able to properly handle the non-linear mapping from the target's state space to measurement space. For example, ambiguities resulting from array geometry are preserved.

A Bayesian approach also provides a simple, consistent method for data fusion. That is, all that is required to incorporate a new measurement into the target's state is the generation of an appropriate likelihood function from the measured data and an application of Bayes' rule. This procedure results in a posterior probability density function (PDF) which clearly captures the uncertainty in the target's state. In light of these advantages, the data fusion approach for target tracking used in this thesis is based on a Bayesian inference technique [45].

In practice, the PDF must be approximated using a discrete representation. There are various approaches for this including particle filters [22], ensemble-based representations [27], and grid-based representations [45]. Regardless of the represen-

tation chosen, the PDF is updated in two different ways. A *measurement update* occurs when newly measured data is incorporated into the PDF. A *motion update* is necessary to project the PDF forward in time. These two steps form the backbone of Bayesian tracking.

When multiple signals are present, it is necessary to marginalize the joint likelihood function for all signals to produce a single-signal likelihood function that corresponds to the TOI direction of arrival (DOA) (i.e. bearing). Direct marginalization of the joint likelihood function is usually carried out by taking the expected value with respect to all parameters besides the TOI DOA. When using this technique interfering signals may not be sufficiently suppressed if they are not well localized. To this end, an approximate method for marginalizing the joint likelihood function is presented which uses maximum likelihood estimates in place of nuisance parameters such as signal powers, noise power, and interferer DOAs. The method ensures that interferers are sufficiently suppressed even when there is little *a priori* information regarding their location.

The outline of the remainder of this thesis is as follows. Background on passive sonar signal processing and Bayesian tracking is given in Chapter 2. Chapter 3 then presents the derivation of the single-signal likelihood function. This is followed in Chapter 4 by discussions regarding the utilization of available prior information. Section 4.1 and Section 4.2 present algorithms that utilize prior information when the number of interfering signals is known and unknown, respectively. The algorithm of Section 4.1 is tested against simulated data and performance results are given in the same section. Data measured during the SEABAR 07 [18] sea trial are used to test the performance of the algorithms of Section 4.2. Results are given in Section 4.2.4.3. A conclusion and a discussion of future work on this topic follows in Chapter 5.

Chapter 2

Background

2.1 Model

2.1.1 Physical Model

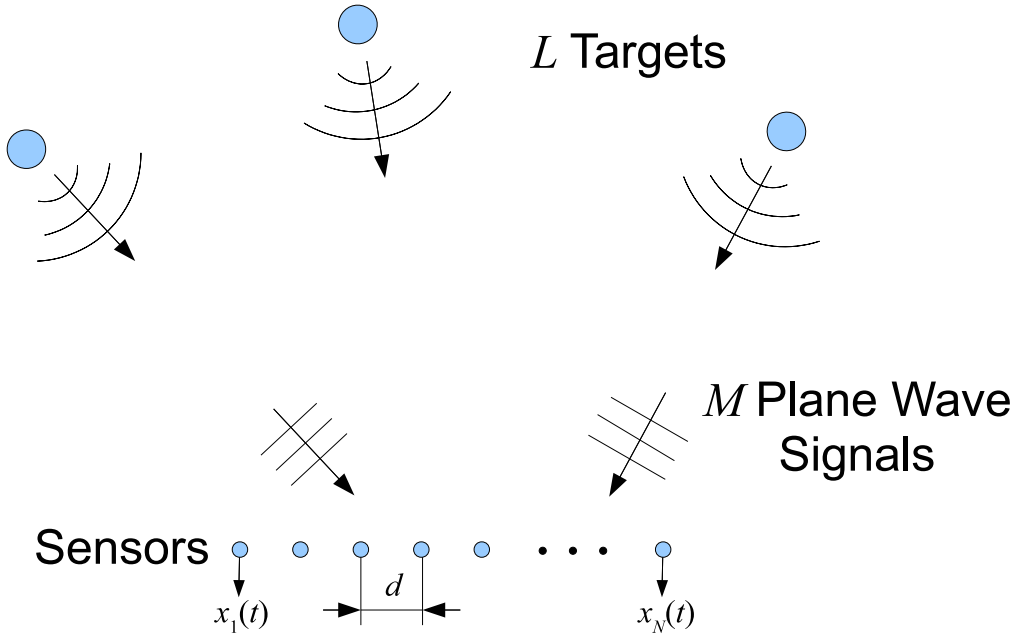

Figure 2.1: An example target and sensor model.

The physical model considered is illustrated in Figure 2.1. There are L targets radiating acoustic pressure signals onto an N-element uniformly-spaced horizontal line array (HLA) with inter-element spacing d. The targets and sensors are assumed to be in the same plane and the signal received at each element, r, is represented by $x_r(t)$. Each target is assumed to behave as a point source that emits spherical waves.

In the realm of passive sonar, these targets are often referred to as acoustic *contacts*. The observed signal model for sensor element r is represented by

$$x_r(t) = \sum_{m=1}^{M} s_{m,r}(t, \theta_m(t)) + n_r(t) \tag{2.1}$$

where $s_{m,r}(t, \theta_m(t))$ represents the m^{th} signal with possibly time-varying parameters $\theta_m(t)$ and $n_r(t)$ represents undesired additive noise. The index $m = 1, 2, ..., M$ represents an index over signals. When the inter-element spacing, d, is much smaller than the shortest distance from a sensor to a target then the target is said to be in the far field of the array. Assuming all targets are in the far field of the array, the received signals can be well approximated by planar wavefronts [48]. Note that the number of signals modeled at the array M does not necessarily have to be equal to the number of modeled targets L.

2.1.2 Data Model

In practice, the data at each sensor are sampled and converted to the frequency domain through a discrete Fourier transform (DFT). The signals are all assumed to be narrowband about the same center frequency. That is, their energy is confined to be in only a few frequency bins. The total observation time, T, is divided into K_t smaller time windows or "snapshots" (the term snapshot can also refer to frequency bins). Seperate DFTs are then taken on each time snapshot. It is further assumed that the DOA of each signal is approximately constant over the observation time, T. Given these assumptions, the observed data in a single snapshot can be modeled (in the frequency domain) as an $N \times 1$ vector

$$\mathbf{x}(k_f, k_t) = \sum_{m=1}^{M} s_m(k_f, k_t)\, \mathbf{v}(k_f, \phi_m) + \mathbf{n}(k_f, k_t) \tag{2.2}$$

where k_f represents the frequency snapshot index, k_t is the time snapshot index, $s_m(k_f, k_t)$ are the signal amplitudes, $\mathbf{v}(k_f, \phi_m)$ represents the the so-called array manifold vector to a signal in direction ϕ_m, and $\mathbf{n}(k_f, k_t)$ is additive noise. Processing will be performed on K_f frequency snapshots about the signals' center frequency, resulting in a total of $K \equiv K_f K_t$ data snapshots. A measurement will be represented by the variable $\mathbf{X} = \left\{ \mathbf{x}(k) \,\middle|\, k = 1, 2, ..., K \right\}$ where k represents a generic index over data snapshots.

The array manifold vector represents the phase shift of the signal at each sensor relative to a reference sensor. For a linear array with the first element taken to be the reference element the array manifold vector is represented as [48]

$$\mathbf{v}(\phi_m) = \left[\begin{array}{cccc} 1 & e^{j\frac{2\pi d}{\lambda}\cos(\phi_m)} & \cdots & e^{j(N-1)\frac{2\pi d}{\lambda}\cos(\phi_m)} \end{array} \right]^T \tag{2.3}$$

where the DOA of each signal, ϕ_m, is measured relative to the line of bearing of the array (i.e. 0° is forward endfire and 90° is broadside), λ is the signal wavelength, and $(\cdot)^T$ represents matrix transpose. Here, the line of bearing of the array is defined as the vector originating from element 1 and ending at element N so that element 1 is defined as the forward direction. Frequency dependence has been dropped because it is assumed that the array manifold vector is matched to the signals' center frequency. Note that signal wavelength is related to signal frequency, f, by $\lambda = c/f$ where c is the speed of sound in the surrounding medium.

The design wavelength of a linear array is defined as $\lambda = 2d$, where d is the inter-element spacing. This results in the Nyquist spatial sampling rate of $d = \lambda/2$. If d is decreased so that it is smaller than $\lambda/2$ the signal becomes spatially over-sampled and the array response will tend to have wider beampatterns. If d is larger than $\lambda/2$ the array is spatially under-sampled. Although spatial under-sampling generates

narrower beamwidths (which is advantageous in terms of spatial resolution) it also creates grating lobes which introduce spatial ambiguity, also known as aliasing. That is, the array will be unable to differentiate between the signals coming from two or more directions. The Nyquist spatial sampling rate therefore provides the greatest spatial resolution without introducing spatial aliasing. When $d = \lambda/2$ the upper limit on the number of resolvable signal DOAs is $N - 1$ [49, 1].

A quantity commonly required in many adaptive signal estimation procedures is the sample covariance matrix,

$$\mathbf{C_x} = \frac{1}{K} \sum_{k=1}^{K} \mathbf{x}\left(k\right) \mathbf{x}\left(k\right)^H, \tag{2.4}$$

where $(\cdot)^H$ represents the complex conjugate transpose or "Hermitian transpose". The summation over k can include both time and frequency snapshots. Generally, it is desirable to have as much time and frequency averaging as possible, as it reduces the background noise level and allows for better inversion of $\mathbf{C_x}$ (more on this in Section 2.2.4). Care must be taken, though, not to average over too much time or frequency when forming this quantity. Specifically, the amount of time averaging is limited by the target kinematics. If targets are non-stationary and too much time is averaged than contacts will appear to blur out as energy is present over an interval of DOAs. A common rule of thumb for the amount of time averaging is given by [3, 43]

$$T < \frac{\lambda}{L_{\text{array}} \dot{\phi}} \tag{2.5}$$

where T is the total observation time, $L_{\text{array}} = d\left(N - 1\right)$ is the array aperture length, and $\dot{\phi}$ is the largest expected bearing rate for a contact.

The amount of bandwidth, B, that may be used for frequency averaging is

constrained by the behavior of signals arriving close to array endfire. As signals of different frequencies travel the length of the array they become out of phase. If the bandwidth is too large this will become apparent as a smear of the phase in the sample covariance matrix. Commonly, the bandwidth is constrained by [3, 43]

$$B < \frac{1}{8T_{\text{transit}}} \tag{2.6}$$

where $T_{transit} = L_{\text{array}}/c$ is the transit time across the array at endfire. The approximate number of snapshots available, K, is given by the product of T and B [43].

2.1.3 Statistical Model

It is assumed that the signals and noise are mutually independent, zero-mean Gaussian random processes with variance σ_m^2 and σ_{n}^2, respectively. It is assumed that the additive noise is (spatially and temporally) white noise. It does not consider ambient noise which may be colored. A stochastic signal model is preferred because it almost always outperforms a deterministic signal model [36]. Based on the model of (2.2), and additionally assuming that the signals are uncorrelated, the observation data covariance matrix has the form

$$\begin{aligned} \mathbf{R}_{\mathbf{x}}(\mathbf{s}) &= E\left\{\mathbf{x}(k)\,\mathbf{x}(k)^H\right\} \\ &= \sum_{m=1}^{M} \sigma_m^2 \mathbf{v}(\phi_m)\,\mathbf{v}(\phi_m)^H + \sigma_{\text{n}}^2\mathbf{I} \end{aligned} \tag{2.7}$$

where the *expectation value* is denoted as $E\{\cdot\}$. The values σ_m^2 and σ_{n}^2 also represent the signal and noise powers, respectively, and

$$\mathbf{s} = \left\{\sigma_m^2, \phi_m, \sigma_{\text{n}}^2 \middle| m = 1, 2, ..., M\right\} \tag{2.8}$$

represents the state of all signals and noise. The assumption of uncorrelated signals is often well justified in the realm of passive sonar, particularly in deep water scenarios that lack multipath effects. It is shown in [12] that an uncorrelated signals model performs better than a generic signals model (which allows for correlation) when the signals actually are uncorrelated.

The observation data covariance matrix can also be rewritten as

$$\mathbf{R}_{\mathbf{x}}(\mathbf{s}) = \sigma_{m'}^2 \mathbf{v}(\phi_{m'}) \mathbf{v}(\phi_{m'})^H + \mathbf{R}_{\mathrm{n+i},m'} \tag{2.9}$$

where

$$\mathbf{R}_{\mathrm{n+i},m'}(\mathbf{s}_{\mathrm{n+i},m'}) \equiv \sum_{\substack{m=1 \\ m \neq m'}}^{M} \sigma_m^2 \mathbf{v}(\phi_m) \mathbf{v}(\phi_m)^H + \sigma_{\mathrm{n}}^2 \mathbf{I}. \tag{2.10}$$

This grouping of terms is meant to indicate that for a given signal of interest (SOI), say $m = m'$, the remaining signals $m \neq m'$ can be absorbed into an effective noise-plus-interference covariance matrix. That is, with respect to the detection and estimation of signal $m = m'$, the remaining signals behave as interferers. The state of the noise and interferer signals with respect to signal m' is represented by

$$\mathbf{s}_{\mathrm{n+i},m'} = \left\{ \sigma_m^2, \phi_m, \sigma_{\mathrm{n}}^2 \middle| m = 1, 2, ..., M;\ m \neq m' \right\}. \tag{2.11}$$

If it is assumed that snapshots are statistically independent then the joint likelihood function (LF) for receiving the measurement $\mathbf{X}$ given the state $\mathbf{s}$ is given by

$$\begin{aligned} L(\mathbf{X}|\mathbf{s}) &= \prod_{k=1}^{K} \frac{1}{\pi^N |\mathbf{R}_{\mathbf{x}}(\mathbf{s})|} \exp\left[-\mathbf{x}(k)^H \mathbf{R}_{\mathbf{x}}^{-1}(\mathbf{s}) \mathbf{x}(k) \right] \\ &= \pi^{-NK} |\mathbf{R}_{\mathbf{x}}(\mathbf{s})|^{-K} \exp\left[-\sum_{k=1}^{K} \mathbf{x}(k)^H \mathbf{R}_{\mathbf{x}}^{-1}(\mathbf{s}) \mathbf{x}(k) \right]. \end{aligned} \tag{2.12}$$

Using the properties of the matrix trace operator, $\mathrm{tr}(\cdot)$, and removing π^{-NK} because it is a constant independent of $\mathbf{s}$, (2.12) can be rewritten as [48]

$$L(\mathbf{X}|\mathbf{s}) = |\mathbf{R}_{\mathbf{x}}(\mathbf{s})|^{-K} \exp\left\{-K\mathrm{tr}\left[\mathbf{R}_{\mathbf{x}}^{-1}(\mathbf{s})\,\mathbf{C}_{\mathbf{x}}\right]\right\}. \tag{2.13}$$

Often times it is easier to work with the log-likelihood function (LLF). Since the log function, $\ln(\cdot)$, is a monotonically increasing function, maximization of the LLF is equivalent to maximization of the LF. The LLF is found by taking the natural logarithm of (2.13):

$$\ln L(\mathbf{X}|\mathbf{s}) = -K\ln\left(|\mathbf{R}_{\mathbf{x}}(\mathbf{s})|\right) - K\mathrm{tr}\left(\mathbf{R}_{\mathbf{x}}^{-1}(\mathbf{s})\,\mathbf{C}_{\mathbf{x}}\right). \tag{2.14}$$

2.2 Beamforming

Suppose there is interest in estimating the DOA $\phi_{m'}$ of a single signal $s_{m'}(t_k)$ using an array. Typical approaches to bearing estimation often make use of conventional beamforming (or any number of its robust adaptive counterparts [31]), maximum likelihood estimation [8, 13], or subspace methods such as MUSIC [41] and ESPRIT [40]. Beamforming, a method of spatial filtering, is often utilized because of its computational simplicity and its well understood relation to temporal filter theory. The processing is usually done in the frequency domain.

Beamforming is performed by processing each sensor output with a linear time invariant filter. In the frequency domain this amounts to multiplying each sensor output by a complex weight and summing the outputs. The beamforming weights can be stacked into an $N \times 1$ vector, $\mathbf{w}(\phi_{m'})$. Note that when the targets to be estimated are in the far field of the array the beamforming weights are a function of the signal DOA only. An estimate of the desired signal in a particular snapshot is

given by [48]

$$\bar{s}_{m'}(k) = \mathbf{w}(\phi_{m'})^H \mathbf{x}(k) \tag{2.15}$$

where the DOA $\phi_{m'}$ is assumed known. An estimate of the signal power over the measurement $\mathbf{X}$ is given by

$$\bar{\sigma}^2_{m'} = E\left\{|\bar{s}_{m'}(k)|^2\right\} = \mathbf{w}(\phi_{m'})^H \mathbf{C}_{\mathbf{x}} \mathbf{w}(\phi_{m'}) \tag{2.16}$$

where $\mathbf{w}(\phi_{m'})^H \mathbf{C}_{\mathbf{x}} \mathbf{w}(\phi_{m'}) \equiv P(\phi_{m'})$ is referred to as the beamformer output power. When the signal DOA is not known it can be estimated by finding the DOA that maximizes the beamformer output power (assuming it is the loudest signal):

$$\bar{\phi}_{m'} = \max_{\phi_{m'}} P(\phi_{m'}). \tag{2.17}$$

If signal m' does not provide the strongest signal then all of the peaks of $P(\phi_{m'})$ above a specified threshold are found and one is associated with the signal m'. A general narrowband beamformer is shown in Figure 2.2.

2.2.1 Conventional Beamforming

One of the simplest beamforming operations assumes the desired estimation of a single plane wave in the absence of noise and interference. The processor shifts the outputs of each sensor so that they are aligned in time and sums their output. This can be implemented in the time domain by the introduction of a set of time delays at each sensor. A common delay is also added so that the operations are physically realizable (i.e. causal). A normalization factor of $1/N$ is also usually included. This processor, outlined in Figure 2.3, is referred to as a *delay-and-sum beamformer*. It is so prevalent that its use is often simply referred to as conventional beamforming (CBF).

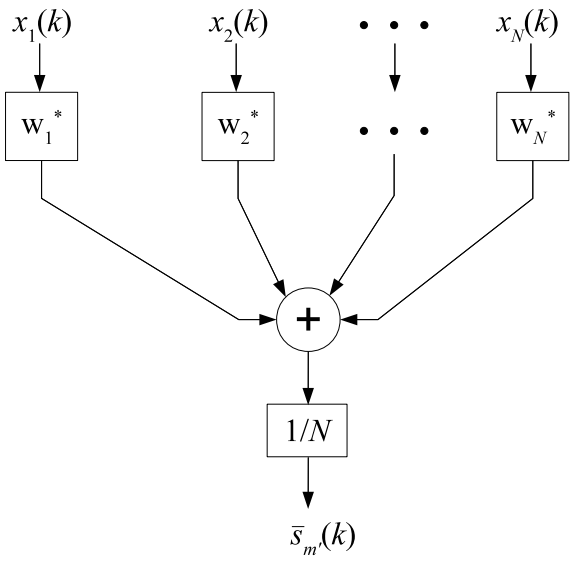

Figure 2.2: A general narrowband beamformer implemented in the frequency domain.

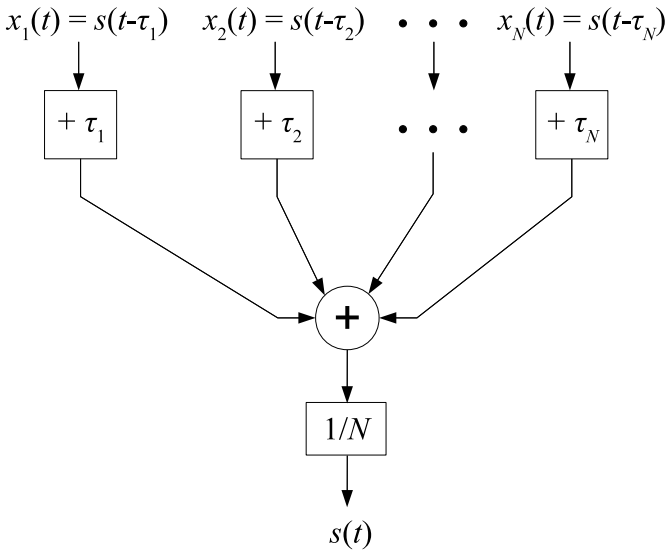

Figure 2.3: A delay-and-sum beamformer implemented in the time domain.

It is usually easier to implement this processor in the frequency domain [48]. In this case, the beamforming weights are given by

$$\mathbf{w}_{\mathrm{CBF}}\left(\phi_{m'}\right) = \frac{1}{N}\mathbf{v}\left(\phi_{m'}\right). \tag{2.18}$$

Here $\mathbf{v}\left(\phi_{m'}\right)$ is referred to as the steering vector to a signal in direction $\phi_{m'}$. The term steering vector is used because the main lobe of the beampattern has been steered to the DOA $\phi_{m'}$. See Figure 2.4 for an example beampattern. The conventional beamformer can also be used in the presence of background noise and interference, but its performance can be severely degraded if loud interferers are present in the sidelobes of the beampattern.

2.2.2 Optimum Beamforming

In many instances there is interest in estimating the DOAs of more than one signal and in signals that are spaced more closely than the classical Rayleigh resolution limit [48]. This can be a very challenging problem for conventional beamforming. Optimum beamformers have been developed that allow for the detection and estimation of multiple closely spaced signals. They assume knowledge of the second order statistics of the data or the noise and interference. When these statistics are not available it is necessary to estimate them from recently measured data. Beamforming that uses these estimated second order statistics is referred to as adaptive beamforming (ABF).

2.2.2.1 Minimum Variance Distortionless Response

One of the most popular optimum beamformers is the minimum variance distortionless response (MVDR) beamformer, originally developed by Capon in his sem-

inal paper, "High-resolution frequency-wavenumber spectrum analysis" [15]. The beamforming weights are found from the solution to

$$\min_{\mathbf{w}} \mathbf{w}^H \mathbf{R}_{\mathrm{n+i},m'} \mathbf{w} \quad \text{subject to} \quad \mathbf{v}\left(\phi_{m'}\right)^H \mathbf{w} = 1. \tag{2.19}$$

That is, it is desired to minimize the estimation error variance subject to a distortionless response in the look direction $\phi_{m'}$. The distortionless response constraint ensures that the estimate of a signal in direction $\phi_{m'}$ will be unbiased. Capon found the solution of this optimization problem to be

$$\mathbf{w}_{\mathrm{MVDR},m'}\left(\phi_{m'}\right) = \frac{\mathbf{R}^{-1}_{\mathrm{n+i},m'} \mathbf{v}\left(\phi_{m'}\right)}{\mathbf{v}\left(\phi_{m'}\right)^H \mathbf{R}^{-1}_{\mathrm{n+i},m'} \mathbf{v}\left(\phi_{m'}\right)}. \tag{2.20}$$

In the absence of interference the MVDR weights become the CBF weights:

$$\lim_{\mathbf{R}_{\mathrm{n+i},m'} \to \sigma^2_{\mathrm{n}} \mathbf{I}} \mathbf{w}_{\mathrm{MVDR},m'}\left(\phi_{m'}\right) = \mathbf{w}_{\mathrm{CBF}}\left(\phi_{m'}\right). \tag{2.21}$$

2.2.2.2 Minimum Power Distortionless Response

The statistics for the noise and interference are not always available. In this case a similar optimum beamformer is often used in which the output power of the beamformer is minimized subject to a distortionless response in the look direction. This filter is referred to as the minimum power distortionless response (MPDR) beamformer and has weights given by

$$\mathbf{w}_{\mathrm{MPDR}}\left(\phi_{m'}\right) = \frac{\mathbf{R}^{-1}_{\mathbf{x}} \mathbf{v}\left(\phi_{m'}\right)}{\mathbf{v}\left(\phi_{m'}\right)^H \mathbf{R}^{-1}_{\mathbf{x}} \mathbf{v}\left(\phi_{m'}\right)}. \tag{2.22}$$

The solution of these weights is identical to that of the MVDR beamformer [15]. MPDR beamforming is usually referred to in the literature as MVDR beamforming despite the different optimization criteria. The term MPDR, suggested by Van Trees

[48], will be used in this thesis to avoid confusion between the two.

2.2.3 Adaptive Beamforming

When second order statistics are unavailable they must be estimated from the data. Capon [15] suggests the use of the sample covariance matrix, $\mathbf{C_x}$, in place of the observation covariance matrix, $\mathbf{R_x}$, when forming the MPDR beamforming weights. This technique is referred to as sample matrix inversion (SMI) and is well justified because $\mathbf{C_x}$ is actually the maximum likelihood estimate (MLE) for an unstructured $\mathbf{R_x}$ [48]:

$$\mathbf{C_x} = \hat{\mathbf{R}}_\mathbf{x} = \frac{1}{K}\sum_{k=1}^{K} \mathbf{x}\left(k\right)\mathbf{x}\left(k\right)^H. \tag{2.23}$$

Similarly, when performing MVDR beamforming it is desired to use an MLE for the noise-plus-interference covariance matrix, $\hat{\mathbf{R}}_{\mathrm{n+i},m'}$, in place of the true $\mathbf{R}_{\mathrm{n+i},m'}$. If the output can be observed without the signal m' present then this estimate can easily be constructed. Unfortunately, this is usually impossible in the realm of passive sonar. A technique for estimating $\hat{\mathbf{R}}_{\mathrm{n+i},m'}$ in the presence of the signal m' is given in Section 3.4.3.3.

2.2.4 Robust Adaptive Beamforming

Adaptive beamformers often have shortcomings that must be addressed in order to achieve robustness. When trying to estimate the DOA of a contact, a finite number of beams are formed that span the full bearing space. To help ensure a constant scalloping loss [32], the beam maximum response axes (MRAs) are spaced equally in u-space [48], i.e. the cosine of the bearing where $u = \cos\left(\phi\right)$. Each beam should be able to "see" signals that arrive at an interval of DOAs between the two adjacent beams.

The MPDR beamformer can suffer from signal suppression and the "squinting effect" if a steered beam is mismatched from the true signal DOA [17]. Signal suppression occurs because the sample covariance matrix is contaminated by the signal of interest (SOI), where the SOI is defined to be the signal we are currently trying to estimate. The beamformer will try to suppress the signal because its goal is to minimize the output power. This has the secondary effect of "squinting" in which a greater-than-unity beampattern response appears to one side of the contact when the beam MRA is not perfectly matched to the true DOA. These effects become stronger as the SOI becomes louder.

MVDR beamforming does not suffer the above effects because the noise-plus-interference matrix is not contaminated by the SOI. Its use is thus always preferred over MPDR whenever a reasonable estimate of the noise-plus-interference matrix can be formed. MVDR and MPDR do share one other weakness. Both beamformers require the computation of the inverse of a covariance matrix ($\mathbf{R}_{\mathrm{n+i},m'}$ for MVDR and $\mathbf{C}_{\mathbf{x}}$ for MPDR). These matrices are only invertible if they are of full rank. For $\mathbf{C}_{\mathbf{x}}$ this requires that $K > N$. As discussed in Section 2.1.2 K is limited by the target dynamics and available bandwidth.

One of the most popular methods for adding robustness to ABF is diagonal loading [16]. This is a procedure which artificially adds spatially-white noise to the covariance matrix when computing the beamforming weights. It has the advantage of decreasing signal suppression and allowing matrix inversion when the number of available snapshots is such that $K < N$. It has the adverse effect of decreasing the resolvability of closely spaced signals [17]. Other methods for robust adaptive beamforming include the addition of point and derivative constraints when forming the beamforming weights, white noise gain constraints [16], covariance matrix tapers

[23], and a myriad of other methods [31].

2.2.5 Beamforming Example

A beamforming example is now considered. The frequency of interest is 200 Hz and the array has $N = 26$ elements and an inter-element spacing of $d = 3.75$ m ($d = \lambda/2$). A 30 second scan was processed with a sampling rate of 2000 Hz and 4096 point FFT windows. Three frequency bins were also shared when computing the sample covariance matrix. This resulted in a total of $K = 42$ snapshots. The SOI has signal power just above the minimum detectable level (MDL), which is roughly $\sigma_{\text{n}}^2/(NK)$, and is located at 80°. Two interferers are located at 40° and 150°. They have signal power 10 dB louder than the SOI. It is assumed that the noise-plus-interference matrix is known a priori.

Shown in Figure 2.4 is the beampattern for various beamformers. It is clear that CBF makes no effort to null out the loud interferers. MVDR beamforming properly places nulls at the locations of the two interferers but maintains a response similar to CBF in regions away from the interferers. The MPDR beamformer also places nulls at the locations of the interferers, but they are not as deep as for the MVDR beamformer. In addition, the response away from the interferers is very different from CBF and MVDR because the optimization criteria is to minimize the total output power. MPDR will therefore attempt to place its nulls wherever there are peaks in the output power, including random noise peaks.

The output power for the various beamformers is shown in Figure 2.5 for the same scenario. CBF shows peaks at the locations of the TOI and the two interferers. MVDR has a similar response to CBF near the location of the SOI, but the peaks at the two interferers are much narrower because the beamformer is attempting to

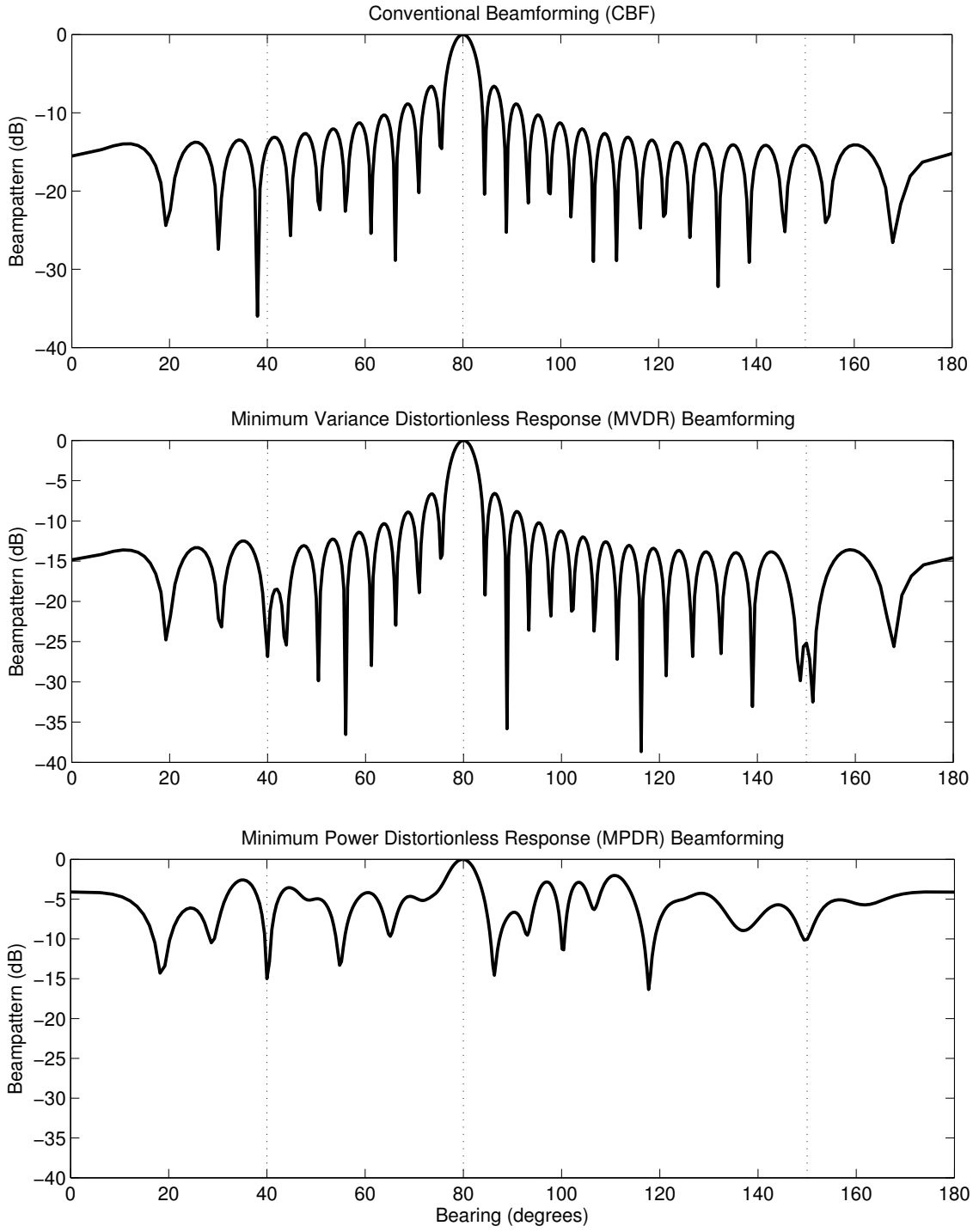

Figure 2.4: Beampatterns for various beamformers. The dotted lines represent the SOI at 80° and two interferers at 40° and 150°.

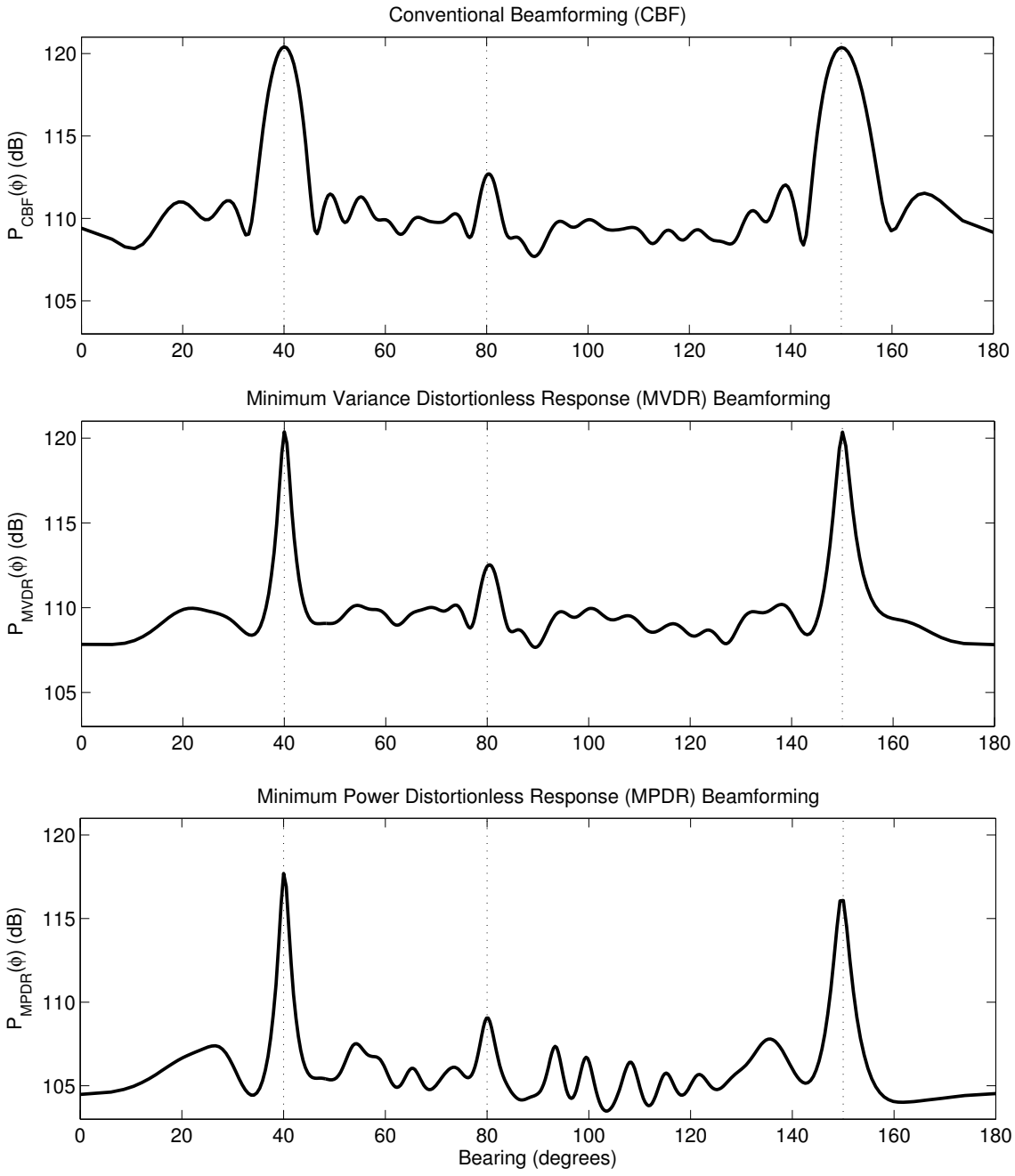

Figure 2.5: Beamformer output power for various beamformers. The dotted lines represent the SOI at 80° and two interferers at 40° and 150°.

null these signals. The MPDR beamformer has a narrower peak at the SOI because it will attempt to null the signal out whenever the beam MRA is mismatched from the true SOI DOA. As one might expect the total MPDR output power is lower than both CBF and MVDR because it is designed to minimize the output power.

2.3 Prior Information

One of the major goals of this work is to exploit available prior information to obtain improved detection and estimation of unknown (or weakly known) targets. Suppose there is interest in tracking a single TOI $l = 1$ in the presence of L total targets. It is assumed that prior information is available regarding the state of this TOI. A scalar p_1 represents the prior probability that the TOI is present and $\rho_1(x_1, y_1)$ represents a prior probability density function (PDF) for the target position given that the TOI is present. Velocity is not included in the PDF because we are focused on TOIs in the far field. The target state space therefore consists of a discrete and continuous portion. The continuous portion, $\rho_1(x_1, y_1)$, is represented in two-dimensional Cartesian coordinates. In practice, this PDF is often discretized to a finite number of grid cells.

Initialization of the prior distribution is an important matter. If no information is available regarding the TOI, a reasonable initialization would be to make $\rho_1(x_1, y_1)$ uniform and to set $p_1 = 0.5$. Although these values work well in many scenarios, we will often assume that the prior PDF contains some refinement in the TOI's position. This is motivated by the fact that much of the author's work has been involved in active-passive data fusion [51, 50, 53, 52]. We therefore assume henceforth that some prior information has been collected in a data fusion framework, either by active sonar state estimates or by previous passive sonar state estimates.

Oftentimes, prior information is available regarding targets other than the TOI. This information may come from a variety of sources, such as a data fusion center, radar, or the Automatic Identification System (AIS) [47]. For the purposes of this thesis, it is assumed that $L-1$ targets other than the TOI are present with unknown probability. These targets will have prior PDFs given by $\rho_l(x_l, y_l)$, $l = 2, 3, ..., L$, and they may or may not interfere with detection and state estimation of the TOI. In addition, it is assumed that these targets emit some amount of measurable acoustic energy at the same frequency as the TOI. The total number of targets is therefore L, where $L-1$ of these targets are potential interferers with respect to the TOI.

Ideally, all collected prior information will be represented in the current state estimate of a TOI. Bayesian inference, which is at the heart of non-linear Bayesian tracking, is the key to obtaining a complete representation of a target's state, and will therefore be the focus of this thesis.

2.4 Bayesian Tracking

In the case of a linear array, the mapping between Cartesian target state space and bearing-only measurement space is non-linear. Ideally, one would like to capture all of the information contained in a measurement in the target's state estimate. This includes information regarding left-right ambiguity and uncertainty due to sidelobes in the array beampattern. A Bayesian approach provides a simple, consistent method for incorporating this information. That is, all that is required to incorporate a new measurement into the target's state is the generation of an appropriate LF from the measured data and an application of Bayes' rule [45]. This procedure results in a posterior PDF which clearly and correctly captures the uncertainty in the target's

state.

Define the index $m^\star$ to be the signal associated with the TOI. The information provided by each measurement of the HLA is given by the LF $L_{m^\star}(\mathbf{X}|\phi_{m^\star})$ (defined in Section 3.1), which represents the probability that the measurement $\mathbf{X}$ would occur given that the signal $m^\star$ is actually at DOA $\phi_{m^\star}$. The state space for the TOI is represented by its position in a two-dimensional Cartesian coordinate system, (x_1, y_1). Although the LF is a function of bearing only, it can be converted to a representation in Cartesian coordinates, $L_{m^\star}(\mathbf{X}|x_1, y_1)$, by assuming no range dependence. By a simple application of Bayes' rule, a new state estimate, $\rho_1(x_1, y_1|\mathbf{X})$ (the posterior PDF), can be formed by combining the previous state estimate, $\rho_1(x_1, y_1)$ (the motion-updated prior PDF), and the LF, $L_{m^\star}(\mathbf{X}|x_1, y_1)$:

$$\rho_1(x_1, y_1|\mathbf{X}) = \frac{L_{m^\star}(\mathbf{X}|x_1, y_1)\,\rho_1(x_1, y_1)}{\int L_{m^\star}(\mathbf{X}|x', y')\,\rho_1(x', y')\,dx'dy'}. \tag{2.24}$$

This step is referred to as the *measurement update* of the Bayesian tracker. Note that implicit in this update is the association of the proper signal $m^\star$ with the TOI $l = 1$. Another important update of the TOI state estimate is the *motion update*. The purpose of the motion update is to project the TOI state estimate forward in time based on known statistics regarding the target dynamics.

The Bayesian tracker used in this thesis is a single target tracker based on the work presented in [27, 28]. Likelihood functions are utilized for target detection as described by the model in [27], while target dynamics are based on an integrated Ornstein-Uhlenbeck process [45]. In addition, a dynamically based birth/death process based on the work of [28] is included. The posterior PDF is approximated using a sampled field approach [45], where the full PDF is represented on a set of fixed sample points in state space. Although the implementation details of the Bayesian

tracker are certainly important, they will not be elaborated upon in this thesis.

Chapter 3

The Single-Signal Likelihood Function

3.1 Statistical Model

When there is only interest in estimating the DOA of a single-signal m' it is convenient to group some of the signal state parameters such that $\mathbf{s} = \{\phi_{m'}, \eta_{m'}\}$ where $\eta_{m'} = \{\sigma^2_{m'}, \mathbf{s}_{\mathrm{n+i},m'}\}$ represents the state of all nuisance parameters. The nuisance parameters in this case include the power of signal m' and the noise and interferer parameters with respect to signal m'. Analysis of (2.10) shows that the majority of the nuisance parameters are contained in the noise-plus-interference covariance matrix.

Given this, it is convenient to rewrite the joint LF, (2.13), so that it is a function of $\phi_{m'}$, $\sigma^2_{m'}$, and $\mathbf{R}_{\mathrm{n+i},m'}$ only. Using the form of (2.9), $|\mathbf{R}_{\mathbf{x}}(\mathbf{s})|$ and $\mathbf{R}^{-1}_{\mathbf{x}}(\mathbf{s})$ can be decomposed as follows [6]:

$$|\mathbf{R}_{\mathbf{x}}(\mathbf{s})| = |\mathbf{R}_{\mathrm{n+i},m'}| \left(1 + \sigma^2_{m'} \mathbf{v}(\phi_{m'})^H \mathbf{R}^{-1}_{\mathrm{n+i},m'} \mathbf{v}(\phi_{m'})\right), \tag{3.1}$$

$$\mathbf{R}^{-1}_{\mathbf{x}}(\mathbf{s}) = \mathbf{R}^{-1}_{\mathrm{n+i},m'} - \frac{\sigma^2_{m'} \mathbf{R}^{-1}_{\mathrm{n+i},m'} \mathbf{v}(\phi_{m'}) \mathbf{v}(\phi_{m'})^H \mathbf{R}^{-1}_{\mathrm{n+i},m'}}{1 + \sigma^2_{m'} \mathbf{v}(\phi_{m'})^H \mathbf{R}^{-1}_{\mathrm{n+i},m'} \mathbf{v}(\phi_{m'})} \tag{3.2}$$

where (3.2) is a result of Woodbury's matrix identity (a special case of the matrix inversion lemma) [48]. Now, substituting $|\mathbf{R}_{\mathbf{x}}(\mathbf{s})|$ and $\mathbf{R}^{-1}_{\mathbf{x}}(\mathbf{s})$ into the joint LF (2.13)

we find

$$L\left(\mathbf{X}|\phi_{m'},\eta_{m'}\right)=\left[\left|\mathbf{R}_{\mathrm{n+i},m'}\right|\left(1+\sigma_{m'}^{2}\mathbf{v}\left(\phi_{m'}\right)^{H}\mathbf{R}_{\mathrm{n+i},m'}^{-1}\mathbf{v}\left(\phi_{m'}\right)\right)\right]^{-K}$$
$$\times\exp\left\{-K\mathrm{tr}\left[\left(\mathbf{R}_{\mathrm{n+i},m'}^{-1}-\frac{\sigma_{m'}^{2}\mathbf{R}_{\mathrm{n+i},m'}^{-1}\mathbf{v}\left(\phi_{m'}\right)\mathbf{v}\left(\phi_{m'}\right)^{H}\mathbf{R}_{\mathrm{n+i},m'}^{-1}}{1+\sigma_{m'}^{2}\mathbf{v}\left(\phi_{m'}\right)^{H}\mathbf{R}_{\mathrm{n+i},m'}^{-1}\mathbf{v}\left(\phi_{m'}\right)}\right)\mathbf{C}_{\mathbf{x}}\right]\right\}. \quad (3.3)$$

Defining $\beta_{m'}\left(\phi_{m'}\right)\equiv\mathbf{v}\left(\phi_{m'}\right)^{H}\mathbf{R}_{\mathrm{n+i},m'}^{-1}\mathbf{v}\left(\phi_{m'}\right)$, which is the denominator of (2.20), and removing the factor $\left|\mathbf{R}_{\mathrm{n+i},m'}\right|^{-K}$ because it is a constant independent of $\phi_{m'}$, (3.3) can be rewritten as

$$L\left(\mathbf{X}|\phi_{m'},\eta_{m'}\right)=\left(1+\sigma_{m'}^{2}\beta_{m'}\left(\phi_{m'}\right)\right)^{-K}$$
$$\times\exp\left\{-K\mathrm{tr}\left[\left(\mathbf{R}_{\mathrm{n+i},m'}^{-1}-\frac{\sigma_{m'}^{2}\mathbf{R}_{\mathrm{n+i},m'}^{-1}\mathbf{v}\left(\phi_{m'}\right)\mathbf{v}\left(\phi_{m'}\right)^{H}\mathbf{R}_{\mathrm{n+i},m'}^{-1}}{1+\sigma_{m'}^{2}\beta_{m'}\left(\phi_{m'}\right)}\right)\mathbf{C}_{\mathbf{x}}\right]\right\}. \quad (3.4)$$

The above equation can be rewritten by using the property that the trace operator is a linear map and that it is invariant under cyclic permutations:

$$L\left(\mathbf{X}|\phi_{m'},\eta_{m'}\right)=\left(1+\sigma_{m'}^{2}\beta\left(\phi_{m'}\right)\right)^{-K}$$
$$\times\exp\left[-K\mathrm{tr}\left(\mathbf{R}_{\mathrm{n+i},m'}^{-1}\mathbf{C}_{\mathbf{x}}\right)+K\sigma_{m'}^{2}\mathrm{tr}\left(\frac{\mathbf{v}\left(\phi_{m'}\right)^{H}\mathbf{R}_{\mathrm{n+i},m'}^{-1}\mathbf{C}_{\mathbf{x}}\mathbf{R}_{\mathrm{n+i},m'}^{-1}\mathbf{v}\left(\phi_{m'}\right)}{1+\sigma_{m'}^{2}\beta\left(\phi_{m'}\right)}\right)\right]. \quad (3.5)$$

The second trace operator may now be removed because the argument is a scalar. Additionally multiplying that argument by $\beta_{m'}\left(\phi_{m'}\right)^{2}/\beta_{m'}\left(\phi_{m'}\right)^{2}$ one obtains

$$L\left(\mathbf{X}|\phi_{m'},\eta_{m'}\right)=\left(1+\sigma_{m'}^{2}\beta\left(\phi_{m'}\right)\right)^{-K}\times\exp\left[-K\mathrm{tr}\left(\mathbf{R}_{\mathrm{n+i},m'}^{-1}\mathbf{C}_{\mathbf{x}}\right)\right]$$
$$\times\exp\left[K\left(\frac{\sigma_{m'}^{2}\beta_{m'}\left(\phi_{m'}\right)^{2}}{1+\sigma_{m'}^{2}\beta_{m'}\left(\phi_{m'}\right)}\right)\left(\frac{\mathbf{v}\left(\phi_{m'}\right)^{H}\mathbf{R}_{\mathrm{n+i},m'}^{-1}\mathbf{C}_{\mathbf{x}}\mathbf{R}_{\mathrm{n+i},m'}^{-1}\mathbf{v}\left(\phi_{m'}\right)}{\beta_{m'}\left(\phi_{m'}\right)^{2}}\right)\right]. \quad (3.6)$$

Noting the form of $\mathbf{w}_{\mathrm{MVDR},m'}\left(\phi_{m'}\right)$ in (2.20) and removing the factor $\exp\left[-K\mathrm{tr}\left(\mathbf{R}_{\mathrm{n+i},m'}^{-1}\mathbf{C}_{\mathbf{x}}\right)\right]$ because it is a constant independent of $\phi_{m'}$, the above sim-

plifies to

$$L\left(\mathbf{X}|\phi_{m'},\eta_{m'}\right) = \left(1+\sigma_{m'}^2\beta_{m'}\left(\phi_{m'}\right)\right)^{-K} \times \exp\left[K\left(\frac{\sigma_{m'}^2\beta_{m'}\left(\phi_{m'}\right)^2}{1+\sigma_{m'}^2\beta_{m'}\left(\phi_{m'}\right)}\right)\mathbf{w}_{\mathrm{MVDR},m'}^H\left(\phi_{m'}\right)\mathbf{C}_{\mathbf{x}}\mathbf{w}_{\mathrm{MVDR},m'}\left(\phi_{m'}\right)\right], \quad (3.7)$$

which contains in it the output power of an MVDR beamformer:

$$L\left(\mathbf{X}|\phi_{m'},\eta_{m'}\right) = \left(1+\sigma_{m'}^2\beta_{m'}\left(\phi_{m'}\right)\right)^{-K} \times \exp\left[K\left(\frac{\sigma_{m'}^2\beta\left(\phi_{m'}\right)^2}{1+\sigma_{m'}^2\beta_{m'}\left(\phi_{m'}\right)}\right)P_{\mathrm{MVDR},m'}\left(\phi_{m'}\right)\right]. \quad (3.8)$$

Finally, the desired joint LLF is found to be

$$\ln L\left(\mathbf{X}|\phi_{m'},\eta_{m'}\right) = -K\ln\left(1+\sigma_{m'}^2\beta_{m'}\left(\phi_{m'}\right)\right) + K\left(\frac{\sigma_{m'}^2\beta_{m'}\left(\phi_{m'}\right)^2}{1+\sigma_{m'}^2\beta_{m'}\left(\phi_{m'}\right)}\right)P_{\mathrm{MVDR},m'}\left(\phi_{m'}\right). \quad (3.9)$$

When the nuisance parameters are assumed to be deterministically known, (3.8) will be referred to as the single-signal LF (SSLF), $L_{m'}\left(\mathbf{X}|\phi_{m'}\right)$, and (3.9) will be referred to as the single-signal LLF (SSLLF), $\ln L_{m'}\left(\mathbf{X}|\phi_{m'}\right)$.

An important special case of (3.9) is for the null case. That is, when the signal m' does not exist ($\sigma_{m'}^2 = 0$ and the number of signals is $M-1$) its LLF is simply a constant given by

$$\ln L_{\emptyset}(\mathbf{X}) = 0. \quad (3.10)$$

This value will be referred to as the no-signal log-likelihood and it is necessary for computing target-present probabilities in a Bayesian tracker [27].

3.2 Single-Signal Likelihood Function in the Absence of Interferers

In the absence of interferers the ambient background noise is assumed to be spatially and temporally white. The following components simplify:

$$\beta_1(\phi_1) = \frac{N}{\sigma_{\mathrm{n}}^2}, \tag{3.11}$$

$$P_{\mathrm{MVDR},1}(\phi_1) = P_{\mathrm{CBF}}(\phi_1). \tag{3.12}$$

Note that the subscript m' has been replaced with $m' = 1$ because there is now only one signal. The SSLLF function then becomes

$$\ln L(\mathbf{X}|\phi) = -K \ln\left(1 + N\frac{\sigma_1^2}{\sigma_{\mathrm{n}}^2}\right) + K\left(\frac{N}{\sigma_{\mathrm{n}}^2} \cdot \frac{N\frac{\sigma_1^2}{\sigma_{\mathrm{n}}^2}}{1 + N\frac{\sigma_1^2}{\sigma_{\mathrm{n}}^2}}\right) P_{\mathrm{CBF}}(\phi). \tag{3.13}$$

This is a very interesting result. When their are no interferers the SSLLF is simply a scaled and shifted version of the output power of a conventional beamformer. How much the LLF is scaled and shifted is dependent on the signal and noise powers. This intuitively makes sense. When the signal-to-noise ratio (SNR) is high the LLF becomes very narrow around the true DOA of the signal, reflecting the fact that their is little uncertainty in the DOA. If the SNR is low the LLF will be broader in order to reflect greater uncertainty in the DOA of the signal. For the null case the signal does not exist ($\sigma_1^2 = 0$) and its LLF is again a constant, given by

$$\ln L_{\emptyset}(\mathbf{X}) = 0. \tag{3.14}$$

3.3 Single-Signal Likelihood Function in the Presence of Interferers

When interfering signals are present the SSLLF is more complicated. It is instructive to investigate the various terms of (3.9). The same scenario as in Section 2.2.5 is considered with the nuisance parameters assumed known a priori. The SOI m' is assumed to be the signal associated with the TOI so that $m' = m^\star$. Define the following terms of the SSLLF (3.9):

$$\alpha_{m'}\left(\phi_{m'}\right) \equiv -K \ln\left(1 + \sigma_{m'}^2 \beta_{m'}\left(\phi_{m'}\right)\right), \tag{3.15}$$

$$\gamma_{m'}\left(\phi_{m'}\right) \equiv K\left(\frac{\sigma_{m'}^2 \beta_{m'}\left(\phi_{m'}\right)^2}{1 + \sigma_{m'}^2 \beta_{m'}\left(\phi_{m'}\right)}\right) P_{\mathrm{MVDR},m'}\left(\phi_{m'}\right). \tag{3.16}$$

In Figure 3.1 the various terms of the SSLLF have been plotted. The component $\beta_{m'}\left(\phi_{m'}\right)$ has valleys at the locations of the interferers and is relatively flat everywhere else. The value in the flat regions is approximately equal to the value of the no interferer case, $\beta_{m'}\left(\phi_{m'}\right) = N/\sigma_{\mathrm{n}}^2$, and the minimum value in a valley is equal to $1/\left(\sigma_i^2 + \sigma_{\mathrm{n}}^2/N\right)$ where σ_i^2 is the signal power of that particular interferer.

The term $\alpha_{m'}\left(\phi_{m'}\right)$ resembles a flipped and scaled version of $\beta_{m'}\left(\phi_{m'}\right)$. The strength of this scaling is dependent on the SOI power. The output power of an MVDR beamformer is contained in the $\gamma_{m'}\left(\phi_{m'}\right)$ term. A peak is seen at the SOI DOA as expected in the beamformer output power, $P_{\mathrm{MVDR},m'}\left(\phi_{m'}\right)$. As seen in Figure 2.5, $P_{\mathrm{MVDR},m'}\left(\phi_{m'}\right)$ also has peaks at the locations of the interferers. These peaks are "pushed down" and become valleys due to the multiplication by the $\beta_{m'}\left(\phi_{m'}\right)$ component.

The total SSLLF contains the sum of $\alpha_{m'}\left(\phi_{m'}\right)$ and $\gamma_{m'}\left(\phi_{m'}\right)$. As seen in Figure 3.2, adding $\alpha_{m'}\left(\phi_{m'}\right)$ to $\gamma_{m'}\left(\phi_{m'}\right)$ effectively raises the valleys in $\gamma_{m'}\left(\phi_{m'}\right)$

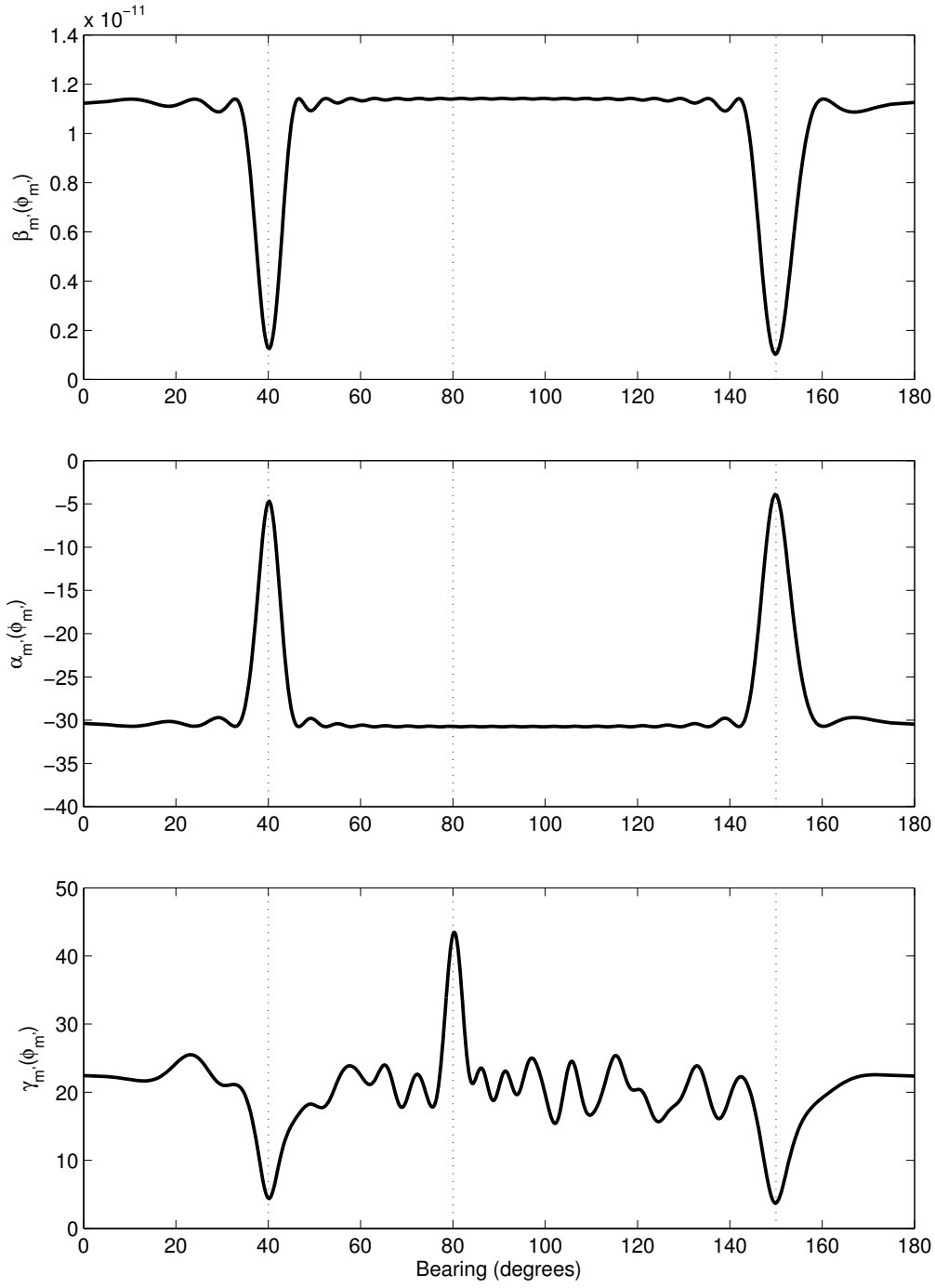

Figure 3.1: Various terms of the single-signal log-likelihood function. The dotted lines represent the SOI at 80° and two interferers at 40° and 150°.

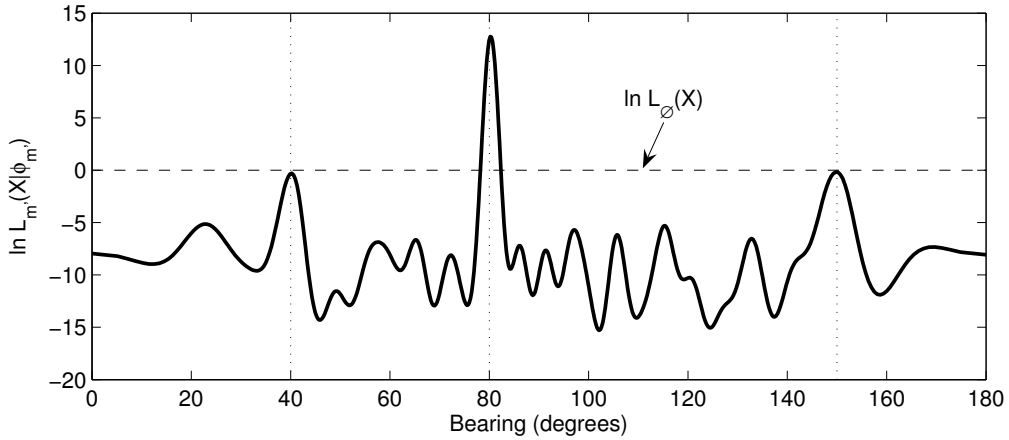

Figure 3.2: The single-signal log-likelihood function. The dotted lines represent the SOI at 80° and two interferers at 40° and 150°. The dashed line represents the no-signal log-likelihood.

closer to the no-signal log-likelihood, where the no-signal log-likelihood is represented by a dashed line. This LLF behaves similarly to the SSLLF without interferers in that the peak will become wider or narrower depending on the SOI SNR. Notice that the peak likelihood occurs at the SOI DOA and that it is above the no-signal likelihood. In this case no other peaks are above the no-signal likelihood. If the SOI power were lower then some other peaks might rise above the no-signal likelihood. This would be representative of added uncertainty in the SOI DOA. The location of these peaks often correspond to sidelobes in the array beampattern.

It is also interesting to discuss the behavior of the SSLLF when knowledge of the nuisance parameters is inaccurate. Error in specific parameters is now considered while the other parameters are considered to be known accurately.

Inaccuracy in the noise power estimate mostly affects signal detection. This is a result of a shift between the SSLLF and the no-signal log-likelihood. If the noise power is overestimated much of the LLF will fall below the no-signal log-likelihood and the target-present probability (of the Bayesian tracker) will drop. Similarly, if

the noise power is underestimated the target-present probability will rise and the localization certainty will generally be overestimated.

Inaccuracy in the interferer signal powers is only detrimental if they are underestimated. When this happens peaks will occur in the SSLLF at their locations above the no-signal log-likelihood. In this case, an interferer may be misidentified as the SOI. The effect is not as bad if the interferer signal powers are overestimated because their peaks in the SSLLF will never rise above the no-signal log-likelihood. This will still wrongfully raise the likelihood at the interferer DOAs, so it is an undesired effect.

Peaks will occur in the SSLLF if the interferer DOAs are not known accurately. This can be attributed to improper nulling of the interferers in the MVDR beamformer. Note that the only data component of the SSLLF is $P_{\text{MVDR},m'}(\phi_{m'})$, which contains in it $\mathbf{C_x}$. Its output will have peaks at the true interferer locations. It is the job of $\beta_{m'}(\phi_{m'})$ and $\alpha_{m'}(\phi_{m'})$, which are a function of the nuisance parameters only, to scale these peaks down to the proper log-likelihood. When the interferer DOAs are inaccurate, $\beta_{m'}(\phi_{m'})$ and $\alpha_{m'}(\phi_{m'})$ will attempt to scale $P_{\text{MVDR},m'}(\phi_{m'})$ at the incorrect DOAs and peaks at the true DOAs will remain. As will be shown later, lack of knowledge in the interferer DOAs introduces a large decrease in performance.

There can also be inaccuracy in the SOI power. Perturbations in this parameter have the general effect of changing the height of the SSLLF peaks at interferers relative to the height of the peak at the SOI. It also changes the overall scale of the LLF (i.e. the dynamic range). An underestimated $\sigma^2_{m'}$ lowers the peaks at interferers and compresses the dynamic range. If the dynamic range is compressed too much the SSLLF will appear flat, causing little change in the TOI state estimate. If $\sigma^2_{m'}$ is overestimated it will raise the peaks at interferers (relative to the SOI peak) and widen the dynamic range, but also push the overall LLF below the no-signal log-likelihood.

This causes the target-present probability to drop.

3.4 Marginalization of the Joint Likelihood Function

3.4.1 Probabilistic Approach

Up to this point the SSLLF has been formed by assuming that the nuisance parameters, $\eta_{m'} = \{\sigma^2_{m'}, \mathbf{s}_{\mathrm{n+i},m'}\}$, are known. In practice, these parameters are not known a priori; that is, they have some uncertainty. They may be estimated from the measured data, but these estimates also have some uncertainty. Their uncertainty may be represented in the form of PDFs, with a uniform PDF representing complete uncertainty in a specific parameter. If a strict probabilistic methodology was followed the SSLF would be formed by taking the expected value of the joint LF with respect to the nuisance parameters:

$$L_{m'}\left(\mathbf{X}|\phi_{m'}\right) = \int_{\eta_{m'}} p\left(\eta_{m'}\right) L\left(\mathbf{X}|\phi_{m'}, \eta_{m'}\right) d\eta_{m'}. \tag{3.17}$$

Unfortunately, even if the nuisance parameters are assumed independent, performing this integration is quite computationally expensive, as it increases non-linearly with the number of signals. In addition, correct marginalization can only be expected when the model order, M, matches the true number of signals.

An example is now considered that shows marginalization of the joint LF using the above approach. The nuisance parameters are assumed to be independent random variables and thus the joint prior PDF may be decoupled as

$$p\left(\eta_{m'}\right) = \left[\prod_{m=1}^{M} p\left(\sigma^2_m\right)\right] \times \left[\prod_{\substack{m=1 \\ m\neq m'}}^{M} p\left(\phi_m\right)\right] \times p\left(\sigma^2_{\mathrm{n}}\right). \tag{3.18}$$

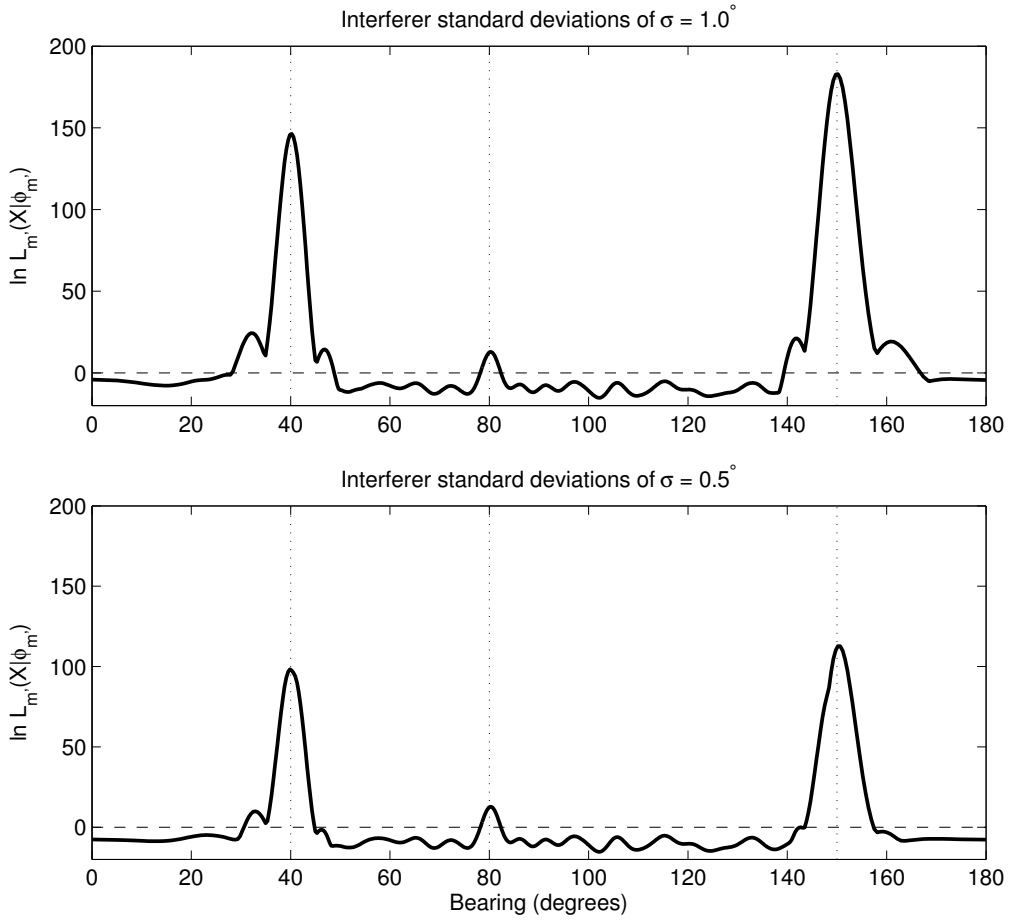

Figure 3.3: Single-signal log-likelihood function marginalized through direct integration. Interferer prior PDFs are insufficiently localized. The dotted lines represent the SOI at 80° and two interferers at 40° and 150°. The dashed line represents the no-signal log-likelihood.

For instructional purposes the signal and noise powers will be assumed known – only uncertainty in the interferer DOAs will be investigated. The scenario is the same as in Section 2.2.5 and Section 3.3. The prior PDFs for the interferer DOAs are assumed to be Gaussian with means at the true DOAs. Various standard deviations are considered. Figure 3.3 shows two scenarios in which the interferer prior PDFs were not localized well enough to remove their influence from the SSLLF. Notice that as the standard deviation of the interferer prior PDFs becomes smaller the interferers become

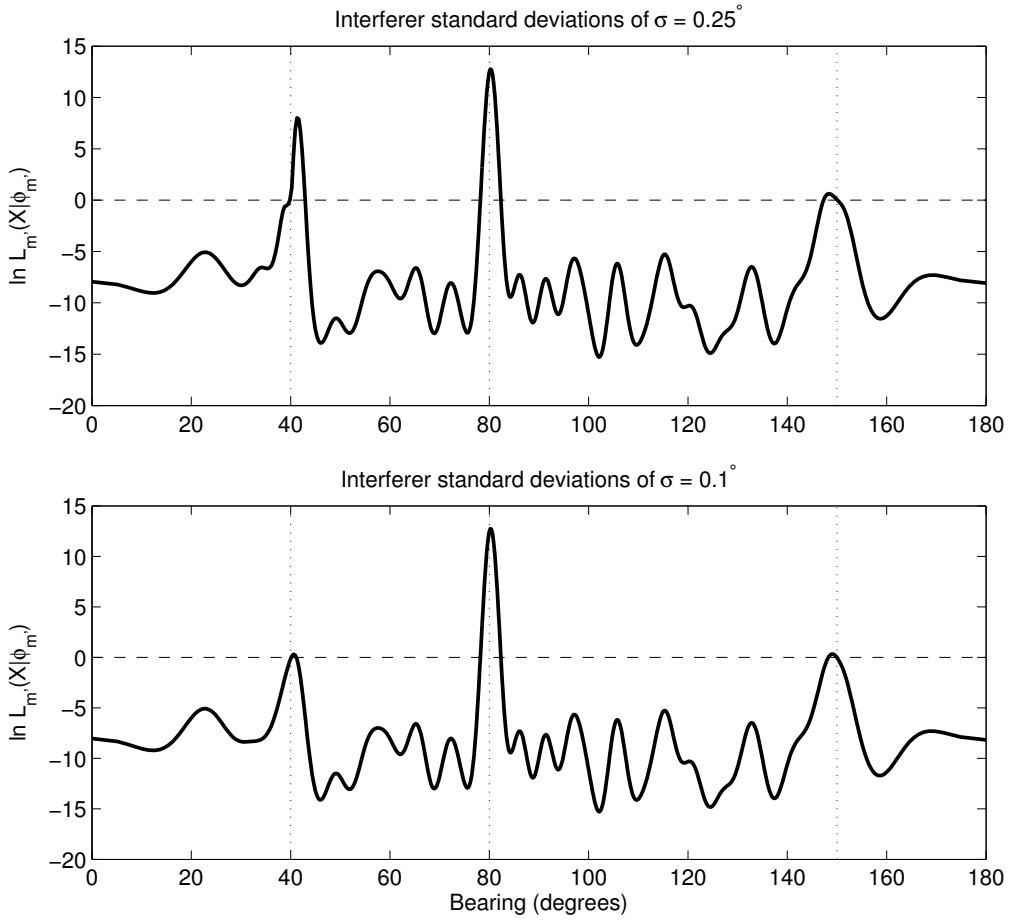

Figure 3.4: Single-signal log-likelihood function marginalized through direct integration. Interferer prior PDFs are sufficiently localized. The dotted lines represent the SOI at 80° and two interferers at 40° and 150°. The dashed line represents the no-signal log-likelihood.

more suppressed. It is only when the standard deviation is below about $\sigma = 0.25°$ that the interferers are suppressed enough to be below the likelihood peak at the SOI. This is seen in Figure 3.4. When the standard deviation is $\sigma = 0.25°$ the interferer peaks are still above the no-signal log-likelihood. This can cause ambiguity in the SOI DOA. It is only when the interferer prior PDFs contain very little uncertainty ($\sigma = 0.1°$) that the interferer peaks fall below the no-signal log-likelihood. As one might expect, the $\sigma = 0.1°$ scenario also approaches the SSLLF for known interferer

DOAs, as seen in Figure 3.2. So, in addition to being computationally restrictive, marginalization of the joint LF via integration will only produce a peak at the SOI when the prior PDFs are very well localized. Although not considered here, an error in the mean estimate of the interferer prior PDFs would produce similar undesirable effects.

3.4.2 Currently Implemented Approximations

One common approach in passive Bayesian tracking is to assume that single DOA "contacts" are received as measurements and that the measurement error is Gaussian in bearing [46, 11]. The LF for each contact then has a Gaussian distribution in bearing from the array. Although this can work as a good approximation, DOA measurement errors are, in general, non-Gaussian. For instance, a Gaussian distribution does not capture the effect of sidelobes in the array beampattern. In addition, this approach requires the association of a single contact with each currently tracked target – a non-trivial problem. Association of the contacts with targets is an approximation to marginalizing the joint LF into several single target LFs.

Another approach to marginalizing the joint LF, first suggested by Bethel [8], is to enforce the condition that signals cannot be coincident (an event indistinguishable from a single signal). The SSLF for a signal $m = m'$ is then formed by multiplying a $M = 1$ hypothesis LF by the "inverse PDFs" of all signals $m \neq m'$, i.e.,

$$L_{m'}\left(\mathbf{X}|\phi_{m'}\right) = L\left(\mathbf{X}|\phi\right) \prod_{\substack{m=1 \\ m\neq m'}}^{M} \left[1 - \frac{L\left(\mathbf{X}|\phi\right)\rho_m\left(\phi\right)}{\int L\left(\mathbf{X}|\phi\right)\rho_m\left(\phi\right)d\phi}\right] \tag{3.19}$$

where $L\left(\mathbf{X}|\phi\right)$ is the $M = 1$ hypothesis LF defined in (3.13) and $\rho_m\left(\phi\right)$ is the prior PDF for signal m. This procedure assumes that all signals have equal element level

SNR and it is conditioned on the presence of signals $m \neq m'$. This marginalization approximation is nearly exact for well separated signals of equal SNR. Since the SNR must be constant in this procedure, it is set as a tuning parameter usually equal to the minimum detectable level (MDL) of the array. This, unfortunately, tends to overestimate the localization uncertainty of signals that have an SNR higher than MDL. In practice, the procedure has to be augmented to include an ad hoc "window" around each signal to ensure that interferers are properly suppressed [42, 10]. This causes the method to not be able to distinguish closely spaced signals. Despite these approximations, this approach has been shown to be quite robust [26].

3.4.3 Proposed Approach

3.4.3.1 Maximum Likelihood Estimation

The marginalization approach taken in this thesis follows the author's previous work [51, 50] in which MLEs (maximum likelihood estimates) $\hat{\eta}_{m'} = \left\{\hat{\sigma}^2_{\mathrm{s},m'}, \hat{\mathbf{R}}_{\mathrm{n+i},m'}\right\}$ are used in place of nuisance parameters:

$$L_{m'}\left(\mathbf{X}|\phi_{m'}\right) = L\left(\mathbf{X}|\phi_{m'}, \hat{\eta}_{m'}\right). \tag{3.20}$$

That is, all parameters in the joint LF, besides the bearing of the SOI, $\phi_{m'}$, are replaced with MLEs. These are found by jointly solving for all MLEs, $\hat{\mathbf{s}}$, in a model order M joint LF. Many methods are available for jointly solving for $\hat{\mathbf{s}}$, including Newton-like search methods [48], the alternating maximization (AM) approach [56], and the expectation maximization (EM) algorithm [19]. The advantage of using MLEs for the nuisance parameters is that the MVDR beamformer in (3.9) places discrete "nulls" in the location of interferers even when there is much uncertainty in the interferer prior PDFs. Uncertainty in the state of signal m' is also correctly

portrayed because MLEs are used for the SNR. The main difficulty of this approach is choosing which signal MLEs to associate with the TOI (target of interest) and which with the interferers. A similar approach to using MLEs for interferer parameters would be to remove the interferers from the data before processing [33].

Most of the maximum likelihood estimation techniques discussed guarantee eventual convergence to the true MLEs, but they do not utilize any prior information. The maximum likelihood estimation approach used in this thesis is the AM approach (also known as the relaxation method in the optimization literature). It is known to be one of the most computationally efficient algorithms [48] and it can be easily adapted to utilize prior information available in a Bayesian tracking framework.

3.4.3.2 Signal and Noise Power Maximum Likelihood Estimates

Two important quantities required for joint maximum likelihood estimation of the signal DOAs are the form of the signal and noise power MLEs. The derivations of these quantities are somewhat lengthy and can be found in [8, 9]. For brevity they will not be included here. The signal power MLE for a particular signal m' is given by

$$\hat{\sigma}^2_{m'}\left(\hat{\phi}_{m'}\right) = \hat{\mathbf{w}}^H_{\mathrm{MVDR},m'}\left(\hat{\phi}_{m'}\right)\left(\mathbf{C_x} - \hat{\mathbf{R}}_{\mathrm{n+i},m'}\right)\hat{\mathbf{w}}_{\mathrm{MVDR},m'}\left(\hat{\phi}_{m'}\right) \tag{3.21}$$

where $\hat{\phi}_m$ are the DOA MLEs, the ML noise-plus-interference matrix with respect to signal m' is

$$\hat{\mathbf{R}}_{\mathrm{n+i},m'}\left(\mathbf{s}_{\mathrm{n+i},m'}\right) = \sum_{\substack{m=1 \\ m\neq m'}}^{M} \hat{\sigma}^2_m \mathbf{v}\left(\hat{\phi}_m\right)\mathbf{v}\left(\hat{\phi}_m\right)^H + \hat{\sigma}^2_{\mathrm{n}}\mathbf{I}, \tag{3.22}$$

and the ML MVDR weights are

$$\hat{\mathbf{w}}_{\mathrm{MVDR},m'}\left(\hat{\phi}_{m'}\right) = \frac{\hat{\mathbf{R}}^{-1}_{\mathrm{n+i},m'}\mathbf{v}\left(\hat{\phi}_{m'}\right)}{\mathbf{v}\left(\hat{\phi}_{m'}\right)^{H}\hat{\mathbf{R}}^{-1}_{\mathrm{n+i},m'}\mathbf{v}\left(\hat{\phi}_{m'}\right)}. \tag{3.23}$$

Solving for the signal power MLE for signal m' requires knowledge of its DOA MLE, the signal power and DOA MLEs for all other signals $m \neq m'$, and the noise power MLE. The noise power MLE is given by

$$\hat{\sigma}^2_{\mathrm{n}} = \frac{1}{N-M}\left[\sum_{n=M+1}^{N} b_{nn} + \left(\sigma^2_{\mathrm{n}}\right)^2 \sum_{n=1}^{M}\left(\frac{b_{nn}}{\left(e_{nn}+\sigma^2_{\mathrm{n}}\right)^2} - \frac{1}{e_{nn}+\sigma^2_{\mathrm{n}}}\right)\right] \tag{3.24}$$

where the eigendecomposition of (2.7) is given by

$$\mathbf{R}_{\mathbf{x}}(\mathbf{s}) = \mathbf{Y}\mathbf{D}\mathbf{Y}^{H} = \mathbf{Y}\mathbf{E}\mathbf{Y}^{H} + \sigma^2_{\mathrm{n}}\mathbf{I} \tag{3.25}$$

and the matrix $\mathbf{B}$ is defined as

$$\mathbf{B} \equiv \mathbf{Y}^{H}\mathbf{C}_{\mathbf{x}}\mathbf{Y}. \tag{3.26}$$

The matrix $\mathbf{Y}$ has columns corresponding to the eigenvectors of $\mathbf{R}_{\mathbf{x}}(\mathbf{s})$, and the diagonal of matrix $\mathbf{E}$ contains the eigenvalues of the signal component of $\mathbf{R}_{\mathbf{x}}(\mathbf{s})$. The nth element of the diagonal of $N \times N$ matrices $\mathbf{E}$ and $\mathbf{B}$ is given by e_{nn} and b_{nn} respectively. In order to solve for the noise power MLE an estimate for the signal parameters must exist, along with a current estimate of the noise power σ^2_{n}. Equation (3.24) can therefore only be used in an iterative mode. The initial noise power MLE used is the mean of the "noise eigenvalues" of $\mathbf{C}_{\mathbf{x}}$; that is,

$$\hat{\sigma}^2_{\mathrm{n}} = \frac{1}{N-M}\sum_{n=M+1}^{N}\epsilon_n \tag{3.27}$$

where ϵ_n are the decreasingly ordered eigenvalues of $\mathbf{C_x}$.

3.4.3.3 Alternating Maximization Algorithm

The alternating maximization (AM) algorithm is used to iteratively solve for the MLEs of all signal and noise parameters. It performs a series of one-dimensional maximizations until convergence to the true MLEs occurs. Presented here is a basic approach that makes no use of prior information, which follows [8]. A model order estimate $\hat{M}$ is determined by selecting a tuning parameter $SNR_{\min}$ that defines the minimum allowable signal-to-noise ratio MLE. Increasingly higher model orders are considered until the ML SNR violates the defined threshold or until the maximum number of resolvable signals is reached. The maximum number of resolvable signals, for a general inter-element spacing $d \leq \lambda/2$, is given by $M_{\max} = (N-1) \times 2d/\lambda$. The implementation details are given in Table 3.1 in the form of pseudocode. If the number of signals is known it can be used in place of $M_{\max}$. As it stands, this algorithm can be computationally restrictive if the model order estimate $\hat{M}$ becomes too large. In some cases prior information can be used to lessen this computational demand while at the same time decreasing the detection and estimation error.

The algorithm produces a set of DOA MLEs $\hat{\phi}_m$ where $m = 1, 2, ..., M$. They are sorted in order of decreasing signal power, as the loudest signals are found first in the AM algorithm because they are the easiest to find [8]. If only a single TOI $l = 1$ is to be tracked then one of these MLEs must be associated with the TOI. This is essentially a problem of data association which will be discussed in Section 4.2. Feedback is utilized in Section 4.1 to perform effective data association.

Select tuning parameter threshold $SNR_{\min}$.

Compute sample covariance matrix $\mathbf{C_x}$.

Initialize model order estimate $\hat{M}$ to 0.

For $M = 1$ to $M_{\max}$

Initialize noise power estimate $\hat{\sigma}^2_{\mathrm{n}}$ using (3.27).

Use (3.22) to form ML noise-plus-interference matrix using estimates from model order $M-1$. Substitute $\hat{\mathbf{R}}_{\mathrm{n+i},M}$ into (3.21) to solve for $\hat{\sigma}^2_M(\phi_M)$ as a function of DOA ϕ_M. Substitute $\hat{\mathbf{R}}_{\mathrm{n+i},M}$ and $\hat{\sigma}^2_M(\phi_M)$ into the joint LLF (3.9) and perform a global search over DOA ϕ_M to maximize the LLF $\ln L\left(\mathbf{X}|\phi_M, \hat{\eta}_M\right)$. Save the DOA estimate $\hat{\phi}_M$ and signal power estimate $\hat{\sigma}^2_M(\hat{\phi}_M)$ that maximize $\ln L\left(\mathbf{X}|\phi_M, \hat{\eta}_M\right)$.

For iteration = 1 to maximum iteration or until maximum LLF converges

Update noise power estimate $\hat{\sigma}^2_{\mathrm{n}}$ using (3.24).

For $m' = 1$ to M

Use (3.22) to form ML noise-plus-interference matrix with respect to signal m'. Substitute $\hat{\mathbf{R}}_{\mathrm{n+i},m'}$ into (3.21) to solve for $\hat{\sigma}^2_{m'}(\phi_{m'})$ as a function of DOA $\phi_{m'}$. Substitute $\hat{\mathbf{R}}_{\mathrm{n+i},m'}$ and $\hat{\sigma}^2_{m'}(\phi_{m'})$ into the joint LLF (3.9) and perform a refined local search over DOA $\phi_{m'}$ to maximize the LLF $\ln L\left(\mathbf{X}|\phi_{m'}, \hat{\eta}_{m'}\right)$. Save the DOA estimate $\hat{\phi}_{m'}$ and signal power estimate $\hat{\sigma}^2_{m'}(\hat{\phi}_{m'})$ that maximizes $\ln L\left(\mathbf{X}|\phi_{m'}, \hat{\eta}_{m'}\right)$.

Next m'

Next iteration

If all $\hat{\sigma}^2_{1:M}/\hat{\sigma}^2_{\mathrm{n}} > SNR_{\min}$, $\hat{M} = M$. Stop search if signals are detected in a non-decreasing order of power.

Next M

Table 3.1: Alternating maximization (AM) algorithm – conventional approach.

Chapter 4

Utilization of Prior Information

4.1 TOI in the Presence of a Known Number of Interferers

4.1.1 Introduction

An interesting approach made possible by data fusion is to use a passive sonar array in a feedback configuration. One type of feedback is the use of the (motion-updated) posterior PDF resulting from one measurement as the prior PDF for a subsequent measurement. This prior PDF can be used to guide the search for the SOI MLEs. In a similar way, known interferers may have prior PDFs that can help guide the search for interferer MLEs. One method of utilizing prior PDFs, presented here, is cued beamforming [52, 53]. An additional layer of feedback can be introduced by using MLEs from a previous measurement as initial guesses for the MLEs of the current measurement. It is important to analyze this scenario because passive sonar typically receives measurements at a faster rate than active sonar. A passive sonar may therefore operate in self feedback for the majority of its operation time, receiving measurement updates from active sonar only occasionally.

This section focuses on the detection and tracking of a single TOI in the presence of a known number of targets that produce interfering signals. It is assumed that the TOI is already associated with a SOI and that the remaining targets are each associated with an interfering signal so that $M = L$. A prior PDF for the TOI is available from a Bayesian tracker. Furthermore, some source besides the Bayesian

tracker has tracked $L-1$ targets that definitely interfere with detection and estimation of the TOI signal. This source likewise provides prior PDFs that describe the location of the interfering targets. MLEs from the previous measurement are also assumed to be available as prior information. In order to assess the performance of the proposed approach, target detection and absolute DOA error are compared to the conventional approach outlined in Table 3.1 that uses no prior information. The proposed approach was first presented by the author in [50].

4.1.2 Cued Beamforming

A global search for MLEs over DOA typically involves sampling the LLF (3.9) with a finite number of beams that span the full bearing space. When prior information regarding the localization of targets exists, one can exploit this knowledge to obtain more accurate state estimates without increasing computational burden.

In [52, 53] an intuitive approach for concentrating (MPDR) beams in areas of high prior probability density was proposed. These *cued beams* were steered within a specified number of standard deviations from the mean of an assumed Gaussian prior PDF. The basic idea behind this approach was to both lower the chance for steering vector mismatch (and hence lessen the chance of signal suppression) and increase sampling resolution in bearing. Doing so allowed for the use of an MPDR beamformer with increased sensitivity. The increased sensitivity corresponds to a decreased need for diagonal loading of the sample covariance matrix. Assuming that the number of cued beams equaled the number of surveillance (i.e. global search) beams, a more accurate and refined bearing estimate could be obtained through an equal expenditure of computational resources. Although advantages were seen in this technique, a continual spacing of MRAs (maximum response axes), based on the

values of the prior PDF $p(\phi)$, would allow for further localization without losing the ability to detect. That is, MRAs should continually change from dense spacing in areas of high prior probability to sparse spacing in areas of low prior probability.

Based on this criterion, a generalized strategy for cueing beams might involve using random samples of the variate ϕ to generate the beam MRAs. This strategy leaves two things to be desired. First, it does not guarantee that the MRAs will span the full range of bearing, from 0° to 180°. Second, it does not have any natural relation to the array geometry. In the case of a HLA, for example, one would like the MRAs to converge to equal spacing in u-space when the prior PDF is uniform (see Section 2.2.4). To this effect, a more intelligent method for choosing the beam MRAs is proposed.

The steps of the cued beamforming algorithm are now outlined. Given a prior PDF in bearing, $\rho(\phi)$, define the following PDF that is a function of u:

$$\rho_u(u) \equiv \frac{\rho(\cos^{-1} u)}{\int_{-1}^{1} \rho(\cos^{-1} u)\, du}. \tag{4.1}$$

This is the PDF that will be sampled to form the cued beams. Next, form the cumulative distribution function (CDF),

$$F_u(u) = \int_0^u \rho_u(t)\, dt \equiv \alpha, \tag{4.2}$$

where $u \in [-1, 1]$ and $F_u(u) = \alpha \in [0, 1]$. If it is assumed that one can solve for the inverse of the CDF, $F_u^{-1}(\alpha) = u$, one can generate a sample of the variate ϕ by randomly generating $\alpha_0 \sim U(0, 1)$, solving $F_u^{-1}(\alpha_0) = u_0$, and converting u_0 to bearing. Although MRAs could be generated using this method, it is instead proposed that the inverse of the CDF in u-space be sampled with J points uniformly-spaced

between zero and one. This results in the set of MRAs,

$$\{\phi_j\} = \cos^{-1}\left[F_u^{-1}\left(\frac{j-1}{J-1}\right)\right], \tag{4.3}$$

where $j = 1, 2, ..., J$. Their are multiple advantages to (4.3), which henceforth are referred to as *cued beams*. First, the cued beams span the full range of bearing, with $\phi_1 = 0^\circ$ and $\phi_J = 180^\circ$ holding true for any prior PDF. In addition, it can be shown that the cued beams and surveillance beams are equivalent for the case of a uniform prior PDF.

It is worth noting that the CDF $F_u(u)$ does not, in general, have an inverse. In practice, though, the prior PDF is approximated by a probability mass function. In this case, inversion amounts to searching a table of F_u for a suitable index, u [39]. In practice, linear interpolation can be used to approximate the index u if it does not exist in the lookup table. Therefore, an approximate inverse CDF can always be generated.

The complexity of computing the cued beams is $O(P)$, where P is the number of points used to approximate the prior PDF. Since this is usually much less than the complexity required for computing the output of an adaptive beamformer, $O(N^3)$, one can say that cued beamforming is of equal computational complexity to surveillance beamforming.

Cued beamforming, in general, can be thought of as adaptive sampling of an objective function when prior information about the parameter of interest is available in the form of a PDF. It can also be compared to the penalty function technique of non-linear programming [7]. That is, although cued beamforming does not assign a penalty to new measurements that are far from expected measurements, sampling the LLF finely in areas of high prior probability and sparsely in areas of low prior

probability essentially lowers the probability of obtaining erroneous measurements, assuming your prior is correct.

Figure 4.1 shows an example of the algorithm for cueing beams. The prior PDF here is a generic, multi-modal distribution, shown in Figure 4.1(a). In (b) the PDF $\rho_u(u)$ is formed. Next, the CDF is generated, as shown by (c). Finally, the inverse CDF is formed in (d) and then sampled uniformly between zero and one ($J = 20$ beams have been chosen for this example). The dotted lines in (d) show the values of u for the generated MRAs. The cued beam MRAs, shown in Figure 4.2, are obtained by taking the inverse cosine of these values.

4.1.3 Feedback of Maximum Likelihood Estimates

The second method of feedback that can be exploited is the use of signal MLEs from the previous measurement as an initial guess for the signal MLEs of the current measurement. The AM algorithm outlined in Table 3.1 can be modified to use this information. It is assumed that signal and noise power MLEs from the previous measurement are available as prior information. Each signal is associated with either the TOI or one of the interfering targets. If it is the first measurement the values must be initialized. There are various ways this could be done. One straightforward method would be to use the expected values of the MPDR beamformer output power for the signal power MLEs:

$$\hat{\sigma}_m^2 = \int_{\phi_m} \rho_m(\phi_m) P_{\text{MPDR}}(\phi_m) \, d\phi_m. \tag{4.4}$$

The noise power MLE can be initialized using the mean of the "noise eigenvalues" of $\mathbf{C_x}$, as defined in (3.27).

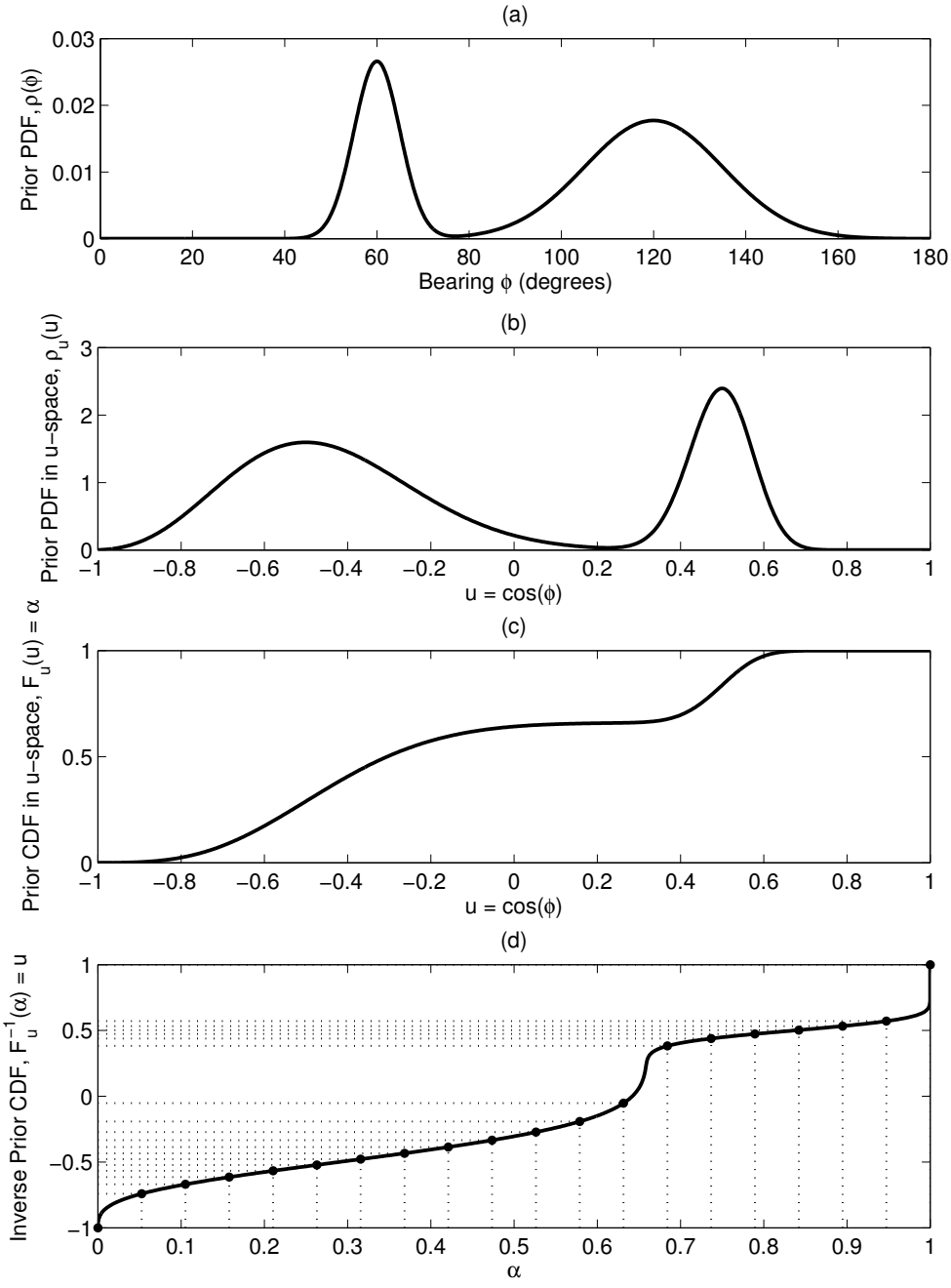

Figure 4.1: An example of the cued beam algorithm. (a) shows the prior PDF in bearing, and (b) shows the prior PDF in u-space. The prior CDF and the inverse of the prior CDF are shown in (c) and (d), respectively. The dotted lines in (d) show the values of u for $J = 20$ generated MRAs.

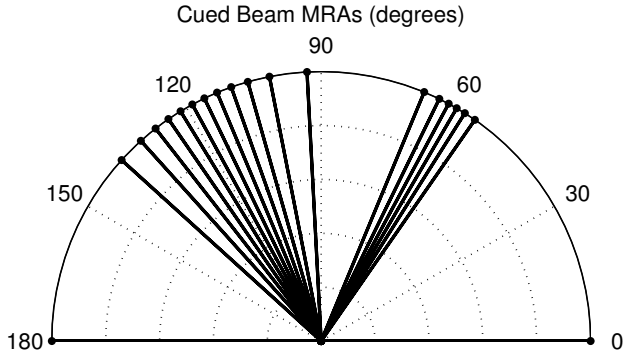

Figure 4.2: Cued Beam MRAs for the prior PDF in Figure 4.1(a).

4.1.4 Proposed Approach

Since the number of interfering targets is assumed known, the full model order, $M = L$, can be used during each MLE search. In other words, there is no need to increment over a hypothesized model order. The number of iterations will also be decreased to one since the MLEs from the previous measurement should already be fairly accurate (although this is not necessary, it will decrease computational demand). For notational simplicity, $\mathbf{X}$ and $\mathbf{X}_0$ are referred to as the current and previous measurement, respectively. The utilization of prior information allows the signals to be effectively associated with the targets. The proposed approach is outlined in the form of pseudo code in Table 4.1. The approach is quite similar to the conventional AM approach of Table 3.1 except that it exploits prior information collected through previous measurements.

After computing the MLEs the SSLLF $L_{m^\star}\left(\mathbf{X}|\phi_{m^\star}\right) = L\left(\mathbf{X}|\phi_{m^\star}, \hat{\eta}_{m^\star}\right)$ may be formed, where $m^\star$ is the signal associated with the TOI. This is the likelihood function that is used to perform a measurement update within the single target Bayesian tracker. MLEs for all signal parameters will be saved for the next measurement. The MAP estimate of the motion-updated posterior PDF will be used as the initial

Compute sample covariance matrix $\mathbf{C_x}$.

Sort signals from measurement $\mathbf{X}_0$ in order of decreasing signal power. Assign indices $m = 1, 2, ..., M$ so that index $m = 1$ corresponds to the highest signal power MLE. Note that one signal $m^\star$ is always associated with the TOI $l = 1$.

Update noise power estimate $\hat{\sigma}^2_{\mathrm{n}}$ using (3.27). Use the signal and noise power MLEs from measurement $\mathbf{X}_0$ and maximum a posteriori (MAP) estimates for the DOA of each target.

For $m' = 1$ to M

> Use (3.22) to form ML noise-plus-interference matrix with respect to signal m'. When computing $\hat{\mathbf{R}}_{\mathrm{n+i},m'}$ use signal power and DOA MLEs from $\mathbf{X}$ for signals $m < m'$ (usually the higher SNR signals); for signals $m > m'$ (usually the lower SNR signals), use signal power MLEs from $\mathbf{X}_0$ and DOA MAP estimates. Substitute $\hat{\mathbf{R}}_{\mathrm{n+i},m'}$ into (3.21) to solve for $\hat{\sigma}^2_{m'}(\phi_{m'})$ as a function of DOA $\phi_{m'}$. Substitute $\hat{\mathbf{R}}_{\mathrm{n+i},m'}$ and $\hat{\sigma}^2_{m'}(\phi_{m'})$ into the joint LLF (3.9) and perform a search over DOA $\phi_{m'}$ using $J = N$ cued beams. Save the DOA estimate $\hat{\phi}_{m'}$ and signal power estimate $\hat{\sigma}^2_{m'}(\hat{\phi}_{m'})$ that maximize $\ln L\left(\mathbf{X}|\phi_{m'}, \hat{\eta}_{m'}\right)$.

Next m'

Table 4.1: Alternating maximization (AM) algorithm – proposed approach with known number of interferers.

DOA estimate for the next measurement. It is assumed that MAP estimates for the interferers are provided by some source besides the single target Bayesian tracker.

4.1.5 Performance Analysis

Simulated data generated by the Sonar Simulation Toolset (SST) [20, 21] was used to assess the effectiveness of the proposed approach in comparison to the conventional AM approach of Table 3.1 that utilizes no prior information. When the conventional AM approach is used it is assumed that proper data association is performed. For the simulation, all targets emitted a steady tone at 200 Hz. A constant sound speed profile of 1500 m/s and a $N = 34$ element HLA of length 45 m were used. Scans of length 12 seconds were processed with a sampling rate of 2400 Hz and 2048 point FFT windows. Three frequency bins were also shared when computing the sample covariance matrix. This resulted in a total of $K = 42$ snapshots. There were a total of 50 scans simulated.

The TOI began at a location of (-9.07, 5.07) km relative to the array and moved with a velocity (6.67, 6.67) m/s for 10 min. It began at a DOA of 151° and ended at 119°. The closest point of approach (CPA) was 10 km. Three different TOI signal levels were considered. The element level SNRs (at CPA) were -12.5 dB, -15 dB, -17.5 dB, and -20 dB. Results were averaged over 100 seperate simulations generated by SST, where the only thing that varied between simulations was the randomness of the background noise.

The TOI state space had dimensions of -20 km to 20 km east-west and 0 to 40 km north-south. The grid size was 51×51 points and the array was placed at (0, 0) km. The array was put at the edge of the state space so that only one side of the array would sample the state space. This removed any left-right ambiguity of the

array and was justified because their was only interest in tracking the DOA of the target, not its range.

First, a moving TOI with no interferers was considered ($M = 1$). The absolute DOA error and target probability are shown as a function of time in Figure 4.3. For each TOI SNR the proposed approach outperforms the conventional AM approach in terms of localization and detection. It is also clear that as the SNR is decreased the target probability also decreases, but maintains a non-zero probability of a target existing. This is reflected by the ability to localize the TOI to within approximately 15° and 35° for the lowest SNRs.

Next, two interferers ($M = 3$) were added with mean locations 10 km from the array at DOAs 60° and 90°. The prior PDF for each of the interferers is Gaussian with equal and uncorrelated x and y variances of 0.25 km^2. The element level SNR for both interferers is 20 dB. Results for this scenario are shown in Figure 4.4. The DOA error performance here is similar to the no-interferers case. Target probability, on the other hand, is noticeably lower when interferers are present. One possible explanation for this is that little likelihood is assigned to TOI DOAs that are nearly co-located with an interferer DOA.

The presented approach shows the ability to track a quiet TOI in the presence of a known number of loud interferers. The need to perform data association is circumvented by utilizing available prior information. Although the proposed approach does not guarantee that the produced MLEs are true MLEs, it is able to obtain comparable or improved performance in comparison to a conventional approach that uses no prior information. This is true even when it is assumed that the conventional AM approach has performed perfect data association. If the data association were less than optimal its performance would further degrade. More importantly, the proposed

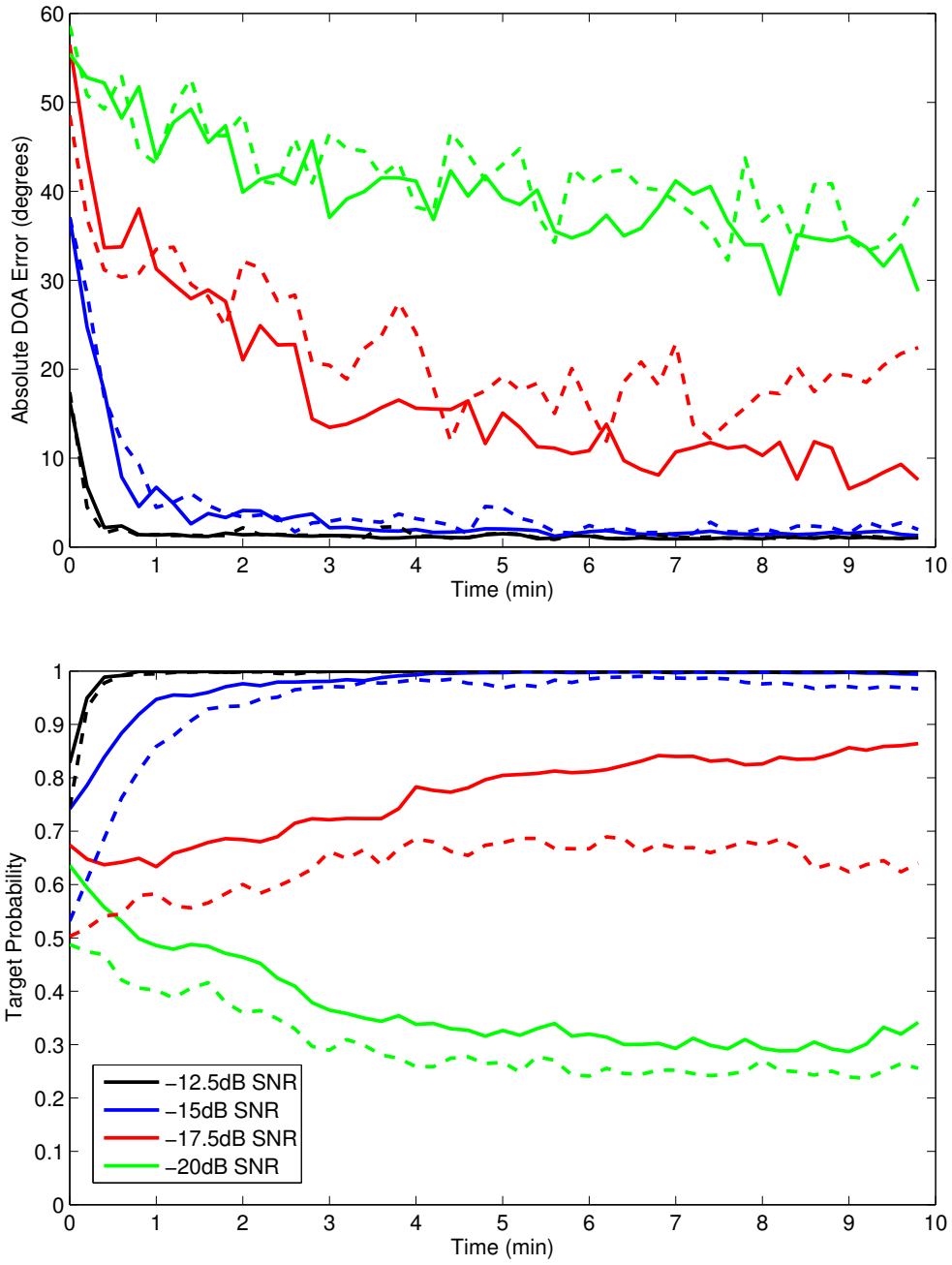

Figure 4.3: Performance of moving target without interferers. The solid lines represent the proposed approach and the dashed lines the conventional alternating maximization (AM) approach.

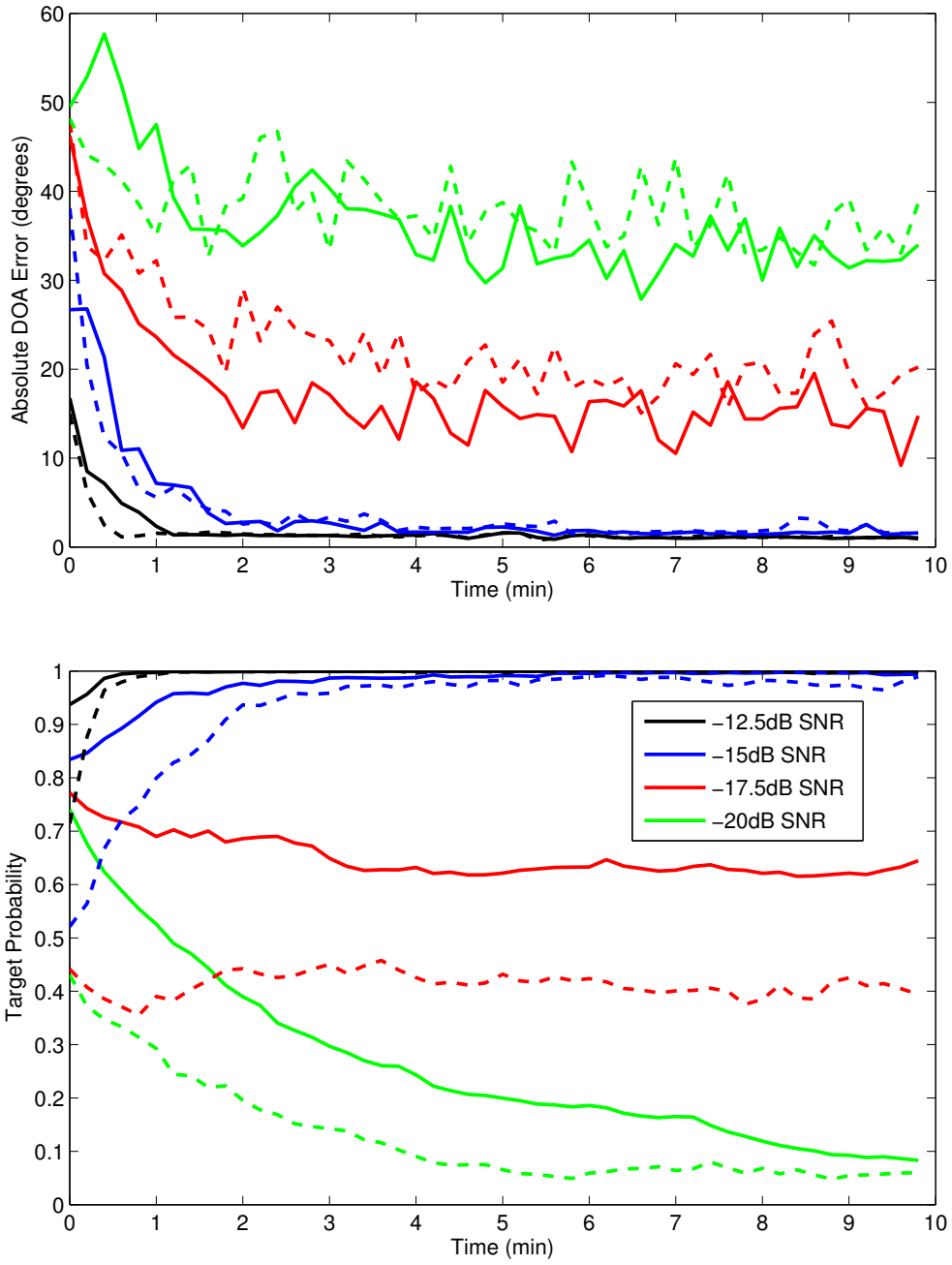

Figure 4.4: Performance of moving target with interferers. The solid lines represent the proposed approach and the dashed lines the conventional alternating maximization (AM) approach.

approach is able to obtain its superior performance with less computational demand than the conventional approach.

4.2 TOI in the Presence of an Unknown Number of Interferers

4.2.1 Introduction

A difficult passive sonar scenario is tracking a single quiet TOI $l = 1$ in the presence of an unknown number of loud interferers. In such a scenario one must either jointly detect and estimate the number of signals (as in Table 3.1) or first perform detection to determine the number of signals, then perform estimation based on this estimate. Joint detection and estimation is usually the preferred approach [48].

Although the conventional AM approach provides a set of M signal DOA MLEs that presumably correspond to M present targets, it does not say which MLE corresponds to each target. Such a problem falls into the realm of data association. If enough prior information is available regarding the location of potentially interfering targets then data association can assign the correct signal MLEs to the TOI.

Prior information should be utilized differently when the number of interfering targets is unknown. Cued beamforming is no longer a viable option because the majority of signal MLEs will never be associated with a target. On the other hand, MLEs from a previous measurement can still be used as initial estimates for the current measurement in order to speed up convergence. The most important use of prior information is the utilization of the target prior PDFs during computation of the association probabilities.

The primary focus of this section is on the detection and tracking of a single TOI $l = 1$ in the presence of an unknown number of interfering signals. It assumes

that a prior PDF for the TOI is available from a Bayesian tracker. In addition, it is assumed that some source besides the Bayesian tracker has tracked $L-1$ potentially interfering targets and can provide prior information regarding their location in the form of prior PDFs. There are therefore a total of L targets representing the location of L possible signals. Signal MLEs from the previous measurement are also assumed to be available as prior information. For simplicity and clarity in presentation it will be assumed that $M = L$; that is, the number of modeled signals is equal to the number of tracked targets. This assumption will be in effect even when not all M signals interfere with detection and estimation of the SOI. Although not considered here, many of the results can be generalized to the case $M \neq L$. An earlier form of the proposed approach was presented by the author in [51].

4.2.2 Data Association

4.2.2.1 Discussion

Data association is a ubiquitous problem in multiple target tracking. As discussed in Section 3.4.1, when measurements are represented as having many "contacts" each contact must be associated with one of the targets being tracked. Since here there is interest in tracking only a single TOI, only one contact would need to be associated with the TOI.

For the purposes of data association, signal DOA MLEs will be treated as contacts, one of which will be associated with the TOI. The signal DOA MLEs are defined as $\hat{\Phi} \equiv \left(\hat{\phi}_1, \hat{\phi}_2, ..., \hat{\phi}_M\right)$. The bearings of all targets are represented by random variables $\Phi \equiv (\phi_1, \phi_2, ..., \phi_M)$ where ϕ_1 is the bearing of the TOI, and it assumed that $L = M$. Presented here is an approach for associating one of the signal DOA MLEs with the TOI. The remaining $M-1$ signal DOA MLEs will be associated with the

remaining targets $l = 2, 3, ..., M$, but each one will not be assigned to a particular target.

4.2.2.2 Association Probabilities

Assume that prior PDFs for all targets have been marginalized to depend on bearing only and are represented by $\rho_l(\phi_l)$. The probability that a signal DOA MLE $\hat{\phi}_m$ is associated with the TOI DOA, ϕ_1, given the M measured DOA MLEs $\hat{\Phi}$ can be expanded using Bayes' rule:

$$P\left(\hat{\phi}_m \leftrightarrow \phi_1 \middle| \hat{\Phi}\right) = \frac{L\left(\hat{\Phi} \middle| \hat{\phi}_m \leftrightarrow \phi_1\right) P\left(\hat{\phi}_m \leftrightarrow \phi_1\right)}{P\left(\hat{\Phi}\right)}. \tag{4.5}$$

Here, the symbol $\leftrightarrow$ is meant to indicate "associated with". Since the value $P\left(\hat{\Phi}\right)$ is a constant independent of m, (4.5) can be rewritten as

$$P\left(\hat{\phi}_m \leftrightarrow \phi_1 \middle| \hat{\Phi}\right) = C_1 L\left(\hat{\Phi} \middle| \hat{\phi}_m \leftrightarrow \phi_1\right) P\left(\hat{\phi}_m \leftrightarrow \phi_1\right) \tag{4.6}$$

where $C_1 \equiv 1/P\left(\hat{\Phi}\right)$ is a normalizing factor. The same value of m maximizes both (4.6) and (4.5).

First, consider the likelihood of receiving all signal MLEs given that a particular MLE is associated with the TOI, $L\left(\hat{\Phi} \middle| \hat{\phi}_m \leftrightarrow \phi_1\right)$. By conditioning on the possible associations of the remaining MLEs with the remaining targets, the LF can be rewritten as

$$L\left(\hat{\Phi} \middle| \hat{\phi}_m \leftrightarrow \phi_1\right) = \sum_{i:i_1=m} L\left(\hat{\Phi} \middle| \hat{\phi}_m \leftrightarrow \phi_1, \hat{\phi}_{i_2} \leftrightarrow \phi_2, ..., \hat{\phi}_{i_M} \leftrightarrow \phi_M\right) \times \underbrace{P\left(\hat{\phi}_{i_2} \leftrightarrow \phi_2, ..., \hat{\phi}_{i_M} \leftrightarrow \phi_M \middle| \hat{\phi}_m \leftrightarrow \phi_1\right)}_{\approx C_2} \tag{4.7}$$

where each $i = (i_1, i_2, ..., i_M)$ is a permutation of $\{1, 2, ..., M\}$ which represents one unique association of the set of MLEs $\hat{\Phi}$ with random variables Φ. That is, each signal MLE $\hat{\phi}_m$ is only associated with one target random variable ϕ_l. The second factor represents the probability of a particular association of the remaining signal MLEs with the remaining targets given that signal m is associated with target $l = 1$. Since there is no prior information indicating otherwise, it is assumed that these probabilities are roughly equal. The factor may therefore be approximated with a constant, C_2, that is independent of m. By additionally assuming that the measurements and associations are statistically independent, (4.7) can be rewritten as

$$L\left(\hat{\Phi}\left|\hat{\phi}_m \leftrightarrow \phi_1\right.\right) = C_2 L\left(\hat{\phi}_m\left|\hat{\phi}_m \leftrightarrow \phi_1\right.\right) \times \sum_{i:i_1=m} \prod_{l=2}^{M} L\left(\hat{\phi}_{i_l}\left|\hat{\phi}_{i_l} \leftrightarrow \phi_l\right.\right). \tag{4.8}$$

In order to solve for each term on the RHS, condition on the prior probability of each ϕ_l:

$$L\left(\hat{\phi}_{i_l}\left|\hat{\phi}_{i_l} \leftrightarrow \phi_l\right.\right) = \int L\left(\hat{\phi}_{i_l}\left|\hat{\phi}_{i_l} \leftrightarrow \phi_l, \phi_l\right.\right) \rho_l\left(\phi_l\right) d\phi_l. \tag{4.9}$$

Ideally one would perform this integral for each association, but an approximation can be made by assuming $L\left(\hat{\phi}_{i_l}\left|\hat{\phi}_{i_l} \leftrightarrow \phi_l, \phi_l\right.\right) \approx \delta\left(\hat{\phi}_{i_l} - \phi_l\right)$. In other words, it is assumed that the algorithm for computing the MLEs has very little error. This allows (4.8) to be rewritten as

$$L\left(\hat{\Phi}\left|\hat{\phi}_m \leftrightarrow \phi_1\right.\right) \approx C_2 \rho_1\left(\hat{\phi}_m\right) \sum_{i:i_1=m} \prod_{l=2}^{M} \rho_l\left(\hat{\phi}_{i_l}\right). \tag{4.10}$$

Unfortunately, calculating (4.10) for large M becomes computationally infeasible because the summation over all associations has $(M-1)!$ terms for each m. An approximation for (4.10) can be made by relaxing the constraint that each MLE $\hat{\phi}_m$ can only be associated with one random variable ϕ_l (see Appendix A for details).

This allows the expression to be factored and rewritten as

$$L\left(\hat{\Phi}\left|\hat{\phi}_m \leftrightarrow \phi_1\right.\right) \approx C_2 \rho_1\left(\hat{\phi}_m\right) \prod_{l=2}^{M} \sum_{\substack{j=1 \\ j \neq m}}^{M} \rho_l\left(\hat{\phi}_j\right). \tag{4.11}$$

The approximate expression (4.11) is computationally easier to implement, but it has many more terms than the more accurate expression (4.10). It is shown in Appendix A, though, that the extra terms are negligible for widely spaced targets. Numerical experiments suggest that this approach also works well for closely spaced targets.

The second factor of interest is the probability that the signal DOA MLE $\hat{\phi}_m$ is associated with the TOI $l = 1$, $P\left(\hat{\phi}_m \leftrightarrow \phi_1\right)$. If all signals were observable then the probability of each association would be equal. Unfortunately, coincident signals are intrinsically not observable [8]. Ideally one would relate $P\left(\hat{\phi}_m \leftrightarrow \phi_1\right)$ to the probability of resolution, that is, the probability that the MLE $\hat{\phi}_m$ is resolvable from other MLEs given that it is associated with target $l = 1$ and that the other MLEs are associated with the remaining targets $l = 2, 3, ..., M$. The probability of resolution for the MPDR beamformer has been calculated by Richmond [38], but to the author's knowledge there have been no published derivations of the resolution probabilities for a multi-signal maximum likelihood estimation technique.

Since the desired effect of this factor is to have low association probabilities when the SOI DOA MLE is located in an area of high prior probability of the potentially interfering targets, the following heuristic form for $P\left(\hat{\phi}_m \leftrightarrow \phi_1\right)$ is proposed:

$$P\left(\hat{\phi}_m \leftrightarrow \phi_1\right) = \prod_{l=2}^{M}\left[1 - g_{l,\hat{i}_m}\right]. \tag{4.12}$$

It is important to note that in practice the prior PDFs are approximated by a probability mass function (PMF) that represents the PDF on a set of discrete points, $\{\phi_i\}$,

uniformly spaced in u-space. Each PMF may be represented as a set of weights given by

$$g_{l,i} = \frac{\rho_l(\phi_i)}{\sum_j \rho_l(\phi_j)} \tag{4.13}$$

where

$$g_{l,\hat{i}_m} \equiv \frac{\rho_l\left(\hat{\phi}_m\right)}{\sum_j \rho_l(\phi_j)} \tag{4.14}$$

and it is assumed that each $\hat{\phi}_m$ is an element of $\{\phi_i\}$. A PMF has the property that $\sum_i g_{l,i} = 1$ and $\max|g_{l,i}| \leq 1$. The factor $\left[1 - g_{l,\hat{i}_m}\right]$ is therefore large (≈ 1) when $\hat{\phi}_m$ is in areas where the prior probability for interferer l is low, and it is small (≈ 0) when $\hat{\phi}_m$ is in areas where the prior probability for interferer l is high. If an interferer l is localized to one PMF cell then an MLE $\hat{\phi}_m$ that falls in this cell would receive zero association probability, $P\left(\hat{\phi}_m \leftrightarrow \phi_1\right)$. The heuristic form of this expression therefore correctly assigns zero association probability when the SOI DOA is coincident with a known interfering target DOA. This approach is quite similar to the data censoring "inverse PDF" approach used by Bethel, Shapo, and Kreucher [8, 42, 26] (see Section 3.4.2), but it performs the data censoring at the data association level instead of the likelihood function level.

Substitution of (4.12) into (4.6) and defining $C \equiv C_1 C_2$ gives the final approximate association probabilities:

$$P\left(\hat{\phi}_m \leftrightarrow \phi_1 \middle| \hat{\Phi}\right) \approx C\rho_1\left(\hat{\phi}_m\right)\left[\prod_{l=2}^{M}\sum_{\substack{j=1 \\ j\neq m}}^{M}\rho_l\left(\hat{\phi}_j\right)\right]\prod_{l=2}^{M}\left[1 - g_{l,\hat{i}_m}\right]. \tag{4.15}$$

The first factor of this expression, $\rho_1\left(\hat{\phi}_m\right)$, rewards a signal DOA MLE if it has high TOI prior probability. The second factor rewards an MLE if the remaining MLEs

closely match the locations of the potentially interfering targets $l = 2, 3, ..., L$. The final factor performs data censoring by penalizing a signal DOA MLE if it closely matches the location of any of the potentially interfering targets. The approximate association probabilities (4.15) can be used to select the most probable association or to perform joint probabilistic data association (JPDA) [5].

There are a few things worth noting about this association procedure. First, the above derivation is conditioned on each target being present. The problem could be generalized to account for targets with known probabilities of being present, but this would greatly increase the computational complexity of calculating the association probabilities. Second, the procedure does not depend on the order in which the signal MLEs are treated, as is common in other methods [35]. That is, each signal is considered and only one is assigned to the TOI. The remaining signals are not assigned to any particular target. Finally, the approximate association probabilities can be easily generalized to the case when the number of tracked targets is not equal to the number of modeled signals ($L \neq M$). In this case (4.15) would become

$$P\left(\hat{\phi}_m \leftrightarrow \phi_1 \middle| \hat{\Phi}\right) \approx C\rho_1\left(\hat{\phi}_m\right) \left[\prod_{l=2}^{L} \sum_{\substack{j=1 \\ j\neq m}}^{M} \rho_l\left(\hat{\phi}_j\right)\right] \prod_{l=2}^{L} \left[1 - g_{l,\hat{i}_m}\right]. \tag{4.16}$$

The $L \neq M$ scenario will not be further investigated in this thesis.

4.2.2.3 Association Techniques

Two techniques of data association are considered in this thesis. The first is maximum association probability data association (MAP DA). In this technique association of a signal MLE with the TOI is obtained by choosing the signal index $m^\star$ that maximizes (4.15). The SSLLF for the TOI is then formed by evaluating (3.9)

with MLEs used in place of nuisance parameters: $\ln L_{m^\star}\left(\mathbf{X}|\phi_{m^\star}\right) = \ln L\left(\mathbf{X}|\phi_{m^\star}, \hat{\eta}_{m^\star}\right)$.

The second technique for performing data association is to use joint probabilistic data association (JPDA) [5]. In this technique the goal is to generate an average posterior PDF for the TOI given the association probabilities. In other words, the effective posterior PDF is given by

$$\rho_{1,\text{eff}}\left(\phi_1\middle|X\right) = \sum_{m=1}^{M} \rho_1\left(\phi_1\middle|X, \hat{\phi}_m \leftrightarrow \phi_1\right) P\left(\hat{\phi}_m \leftrightarrow \phi_1\middle|\,\hat{\Phi}\right). \tag{4.17}$$

Via an application of Bayes' rule, the above expression can be expanded as

$$\begin{aligned}
\rho_{1,\text{eff}}\left(\phi_1\middle|X\right) &= \sum_{m=1}^{M} \frac{\rho_1\left(\phi_1\right) L\left(X\middle|\phi_1, \hat{\phi}_m \leftrightarrow \phi_1\right)}{C_m} P\left(\hat{\phi}_m \leftrightarrow \phi_1\middle|\,\hat{\Phi}\right) \\
&= \rho_1\left(\phi_1\right) \sum_{m=1}^{M} \frac{1}{C_m} L\left(X\middle|\phi_1, \hat{\phi}_m \leftrightarrow \phi_1\right) P\left(\hat{\phi}_m \leftrightarrow \phi_1\middle|\,\hat{\Phi}\right) \\
\rho_{1,\text{eff}}\left(\phi_1\middle|X\right) &= \rho_1\left(\phi_1\right) L_{\text{eff}}\left(X|\phi_1\right)
\end{aligned} \tag{4.18}$$

where

$$L_{\text{eff}}\left(X|\phi_1\right) \equiv \sum_{m=1}^{M} \frac{1}{C_m} L\left(X\middle|\phi_1, \hat{\phi}_m \leftrightarrow \phi_1\right) P\left(\hat{\phi}_m \leftrightarrow \phi_1\middle|\,\hat{\Phi}\right) \tag{4.19}$$

and the constant C_m is defined as $C_m \equiv \int_{\phi_1} \rho_1\left(\phi_1\right) L\left(X\middle|\phi_1, \hat{\phi}_m \leftrightarrow \phi_1\right) d\phi_1$. Examination of (2.24) shows that an average or "effective" likelihood function $L_{\text{eff}}\left(X|\phi_1\right)$ can be used in place of the SSLF $L_{m^\star}\left(\mathbf{X}|\phi_{m^\star}\right)$ when performing the measurement update of the Bayesian tracker.

4.2.3 Proposed Approach

The maximum likelihood estimation algorithm used in this section very closely follows the conventional AM approach of Table 3.1 with a few modifications. First, the signal model order is assumed known. Second, MLEs from the previous measurement

Compute sample covariance matrix $\mathbf{C_x}$.

Sort signals from measurement $\mathbf{X}_0$ in order of decreasing signal power. Assign indices $m = 1, 2, ..., M$ so that index $m = 1$ corresponds to the lowest signal power MLE.

For iteration = 1 to maximum iteration or until maximum LLF converges

For $m' = 1$ to M

Use (3.22) to form ML noise-plus-interference matrix with respect to signal m'. When computing $\hat{\mathbf{R}}_{\mathrm{n+i},m'}$ use signal power and DOA MLEs from $\mathbf{X}$ for signals $m < m'$ (usually the higher SNR signals); for signals $m > m'$ (usually the lower SNR signals), use signal power and DOA MLEs from $\mathbf{X}_0$. Substitute $\hat{\mathbf{R}}_{\mathrm{n+i},m'}$ into (3.21) to solve for $\hat{\sigma}^2_{m'}(\phi_{m'})$ as a function of DOA $\phi_{m'}$. Substitute $\hat{\mathbf{R}}_{\mathrm{n+i},m'}$ and $\hat{\sigma}^2_{m'}(\phi_{m'})$ into the joint LLF (3.9) and perform a localized search over DOA $\phi_{m'}$ based on the iteration number (i.e. perform a more localized and refined search if the iteration number is larger). Save the DOA estimate $\hat{\phi}_{m'}$ and signal power estimate $\hat{\sigma}^2_{m'}(\hat{\phi}_{m'})$ that maximize $\ln L\left(\mathbf{X}|\phi_{m'}, \hat{\eta}_{m'}\right)$.

Next m'

Update noise power estimate $\hat{\sigma}^2_{\mathrm{n}}$ using (3.27). Use the current signal power, DOA, and noise power MLEs.

Next iteration

Table 4.2: Alternating maximization (AM) algorithm – proposed approach with unknown number of interferers.

$\mathbf{X}_0$ are used as initial estimates for the current measurement $\mathbf{X}$. If it is the first measurement, initialization is performed by using the conventional AM approach with M assumed known and no SNR threshold. The proposed algorithm is outlined in form of pseudocode in Table 4.2. Pseudocode is also used to describe the total algorithm for computing the SSLF in Table 4.3.

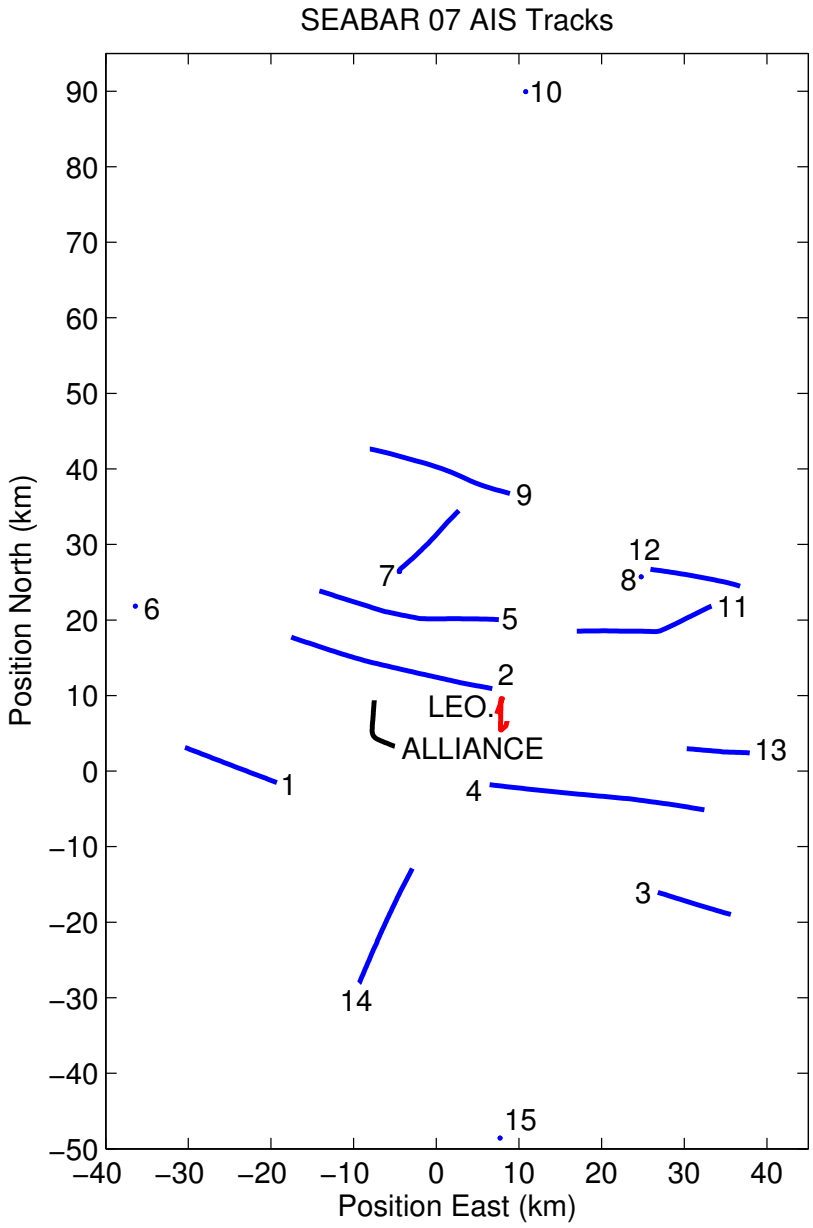

Figure 4.5: SEABAR 07 AIS Tracks for run A01. The Leonardo (the TOI) is in red and the Alliance (pulling the Atlas array) is in black. Blue tracks represent potential interferers. See the legend in Table 4.4 to find the names of the numbered interferers.

Compute signal MLEs by using the alternating maximization (AM) algorithm outlined in Table 4.2. Save all MLEs so they may be used as initial estimates for the next measurement.

Compute association probabilities using (4.15).

If association technique is maximum association probability data association (MAP DA)

> Choose the signal index $m^\star$ which maximizes (4.15). Form the SSLLF for the TOI $\ln L_{m^\star}(\mathbf{X}|\phi_{m^\star}) = \ln L(\mathbf{X}|\phi_{m^\star}, \hat{\eta}_{m^\star})$ by evaluating (3.9) with MLEs used in place of nuisance parameters.

Else association technique is joint probabilistic data association (JPDA)

> Form SSLF $L_{\text{eff}}(X|\phi_1)$ using (4.19) and use it in place of $L_{m^\star}(\mathbf{X}|\phi_{m^\star})$ in the measurement update (2.24).

End

Table 4.3: Total algorithm for computing the single-signal likelihood function – proposed approach with unknown number of interferers.

4.2.4 Performance Analysis

4.2.4.1 Description and Preliminary Analysis of SEABAR 07 Sea Trial

Data measured during run A01 of the SEABAR 07 sea trial [18] were used to assess the performance of the proposed approach. This trial presented itself as a very challenging passive estimation problem. Information regarding the position of 30 vessels was available from the Automatic Identification System (AIS). AIS is an electronic communication system for exchanging useful ship information such as identification, position, course, and speed. To make the analysis more manageable, consideration was limited to the vessels shown in Table 4.4, most of which are the closest vessels to the region of interest. Tracks for these vessels can be seen in Figure 4.5 where the position is shown in kilometers referenced to 36.303°N, 14.7°E latitude-longitude. Subsequent figures will also use this reference. Figure 4.6 shows a bearing

AIS Name	Assigned Number
Leonardo	0
Navajo	1
Waterford	2
Alberta	3
Iran Amol	4
Karavi	5
Avior	6
Kerob	7
MSC Heidi	8
Green Honduras	9
Flaminia	10
Handytankers Unity	11
Mar Daniela	12
Sun Rose	13
Challenger	14
British Falcon	15

Table 4.4: Names of vessels reported by AIS and assigned numbers.

time record (BTR) for these AIS tracks, where angles are referenced to foreward endfire of the array. Times on all plots are referenced to 12:30 Oct. 13, 2007 UT (universal time). In addition, it is assumed that the only targets present are those reported by AIS; that is, there are no unknown targets.

The one receiver used is the Atlas array, which was towed by the research vessel (R/V) Alliance. This HLA is 11.25 m long and contains 126 elements. The design frequency of the array is therefore approximately 8333 Hz. It was towed at a scope of approximately 200 m, for which minor corrections were made in the data. The array was modeled as rigid at all times, which was reasonable given its short length. Finally, the sampling rate of the array is 5000 Hz.

All processing is narrowband about 1008 Hz. Although most of the targets present (including the Leonardo) emitted broadband noise, the Alberta was a loud

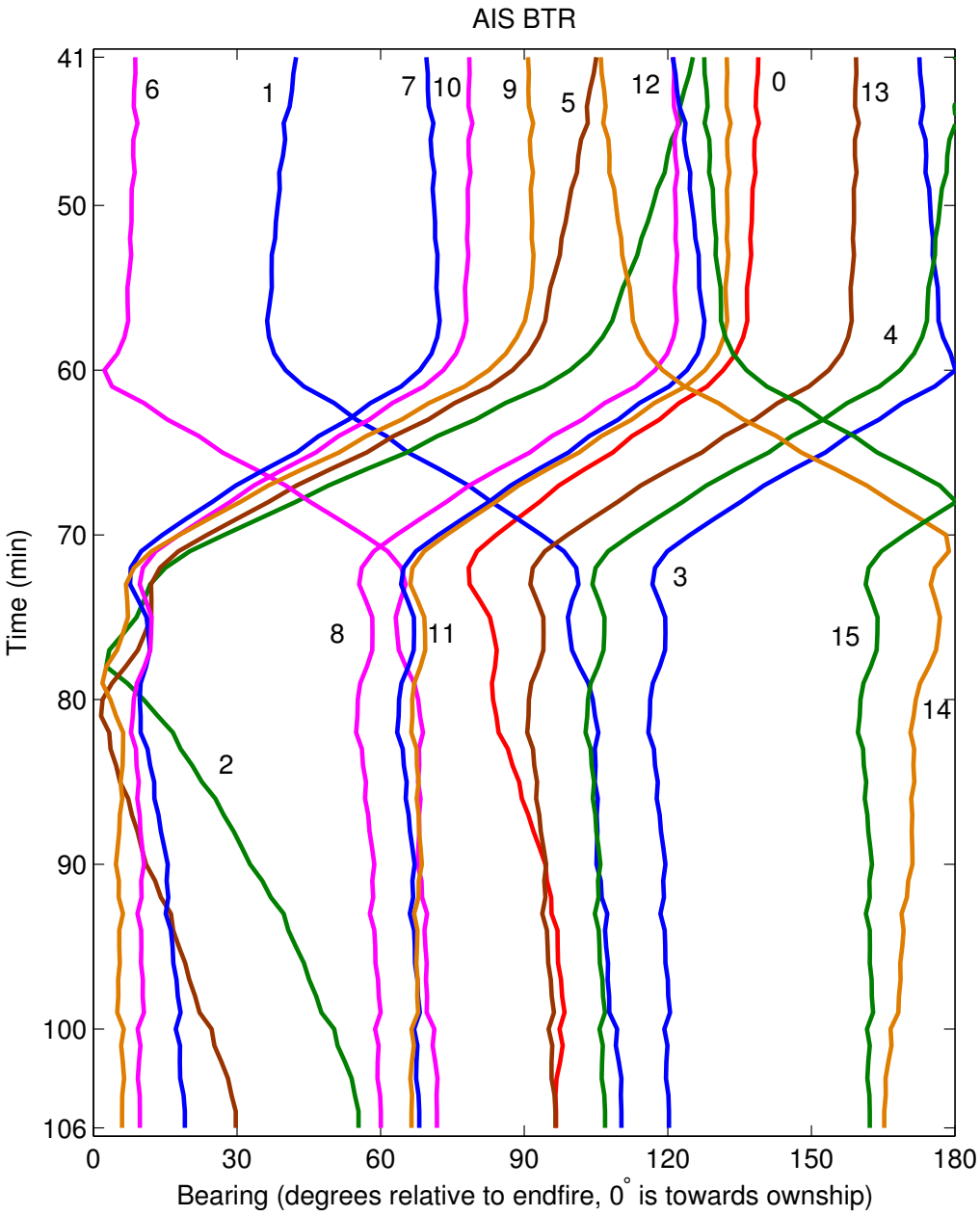

Figure 4.6: BTR showing AIS position information. The Leonardo is shown in red and labeled 0. The tracks for potential interferers are shown in varying colors. See the legend in Table 4.4 to find the names of the numbered interferers.

narrowband interferer emitting at around 1008 Hz. The decision was made to include it in the analyzed data to increase the challenge of tracking the TOI. There were sixty-six one minute scans of data processed. Each scan was processed using 512 point FFT windows. This resulted in about 585 time snapshots per scan. In addition, three frequency bins were shared when computing the sample covariance matrix defined in (2.4).

Although an AIS track was available for the R/V Leonardo, it was chosen as the TOI. This was motivated by the fact that it makes two sharp maneuvers, as seen in Figure 4.7, and that it does not stand out on a narrowband adaptive beamformer BTR plot, as seen in Figure 4.8. In addition, the AIS track provides one source of "truth" against which to evaluate performance. The element-level SNR of the signal from the Leonardo was high enough so that it was easily detected. The main challenge to tracking the Leonardo is in data association. Therefore, no results are shown for target detection.

For comparison purposes, a BTR was also created using subband energy detection processing. Figure 4.9 shows this plot. Processing was done on a frequency band spanning 800-1100Hz. The variant of the processing used was subband peak energy detection – energy detect (SPED ED) [14]. The Leonardo is somewhat visible in this plot, particularly between minutes 50-90. From 90 minutes forward it is difficult to tell whether the track is due to the Leonardo or interferer 13, the Sun Rose.

The dimensions of the state space used to track the Leonardo were from -20 to 20 km east and from -15 to 25 km north. Since the measurements contain only bearing information, it is not of critical importance that all targets be within the boundaries of the state space. The PDF is estimated using a sample grid of 101x101 points. In addition, the prior PDF for the Leonardo was modeled to be uniform with

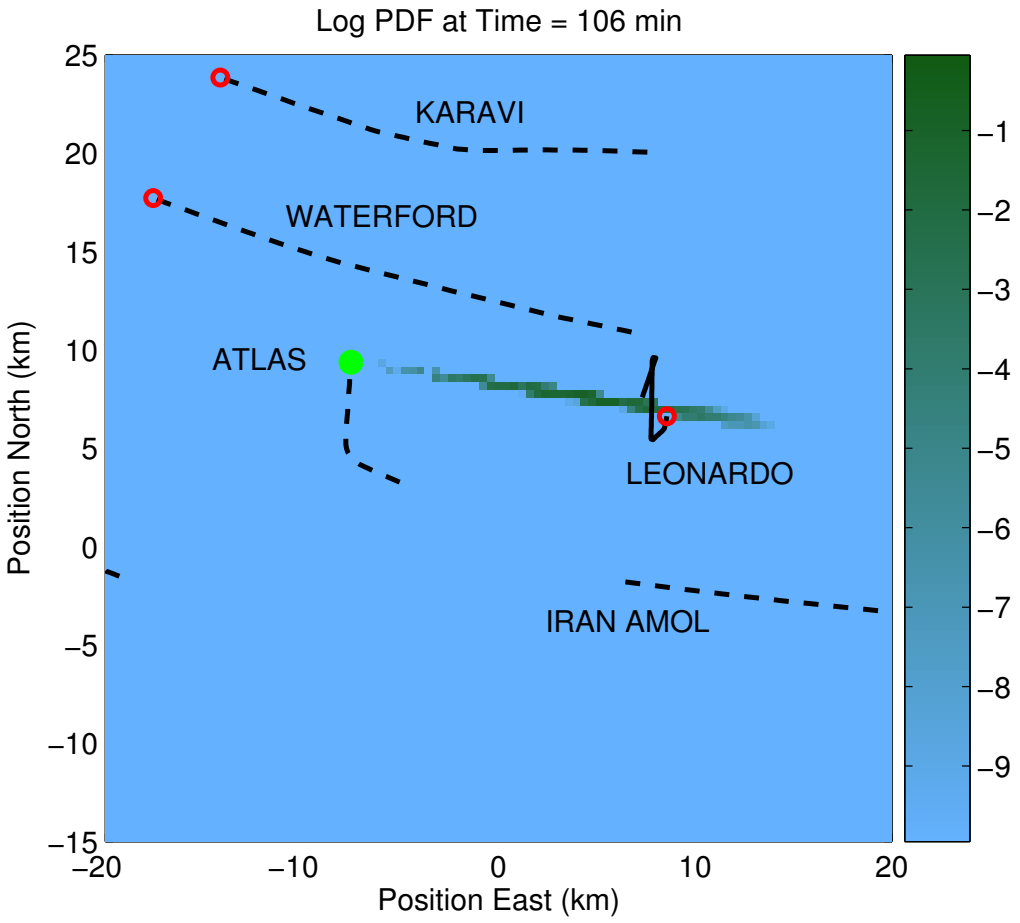

Figure 4.7: Posterior log-PDF for the Leonardo at a time of 106 minutes with targets 1-10 modeled as interferers, ML estimates used for signal powers, and MAP data association performed. The current position of the targets and receivers are shown by circles. Dotted and solid lines show the past trajectories. Notice the sharp maneuvers made by the Leonardo.

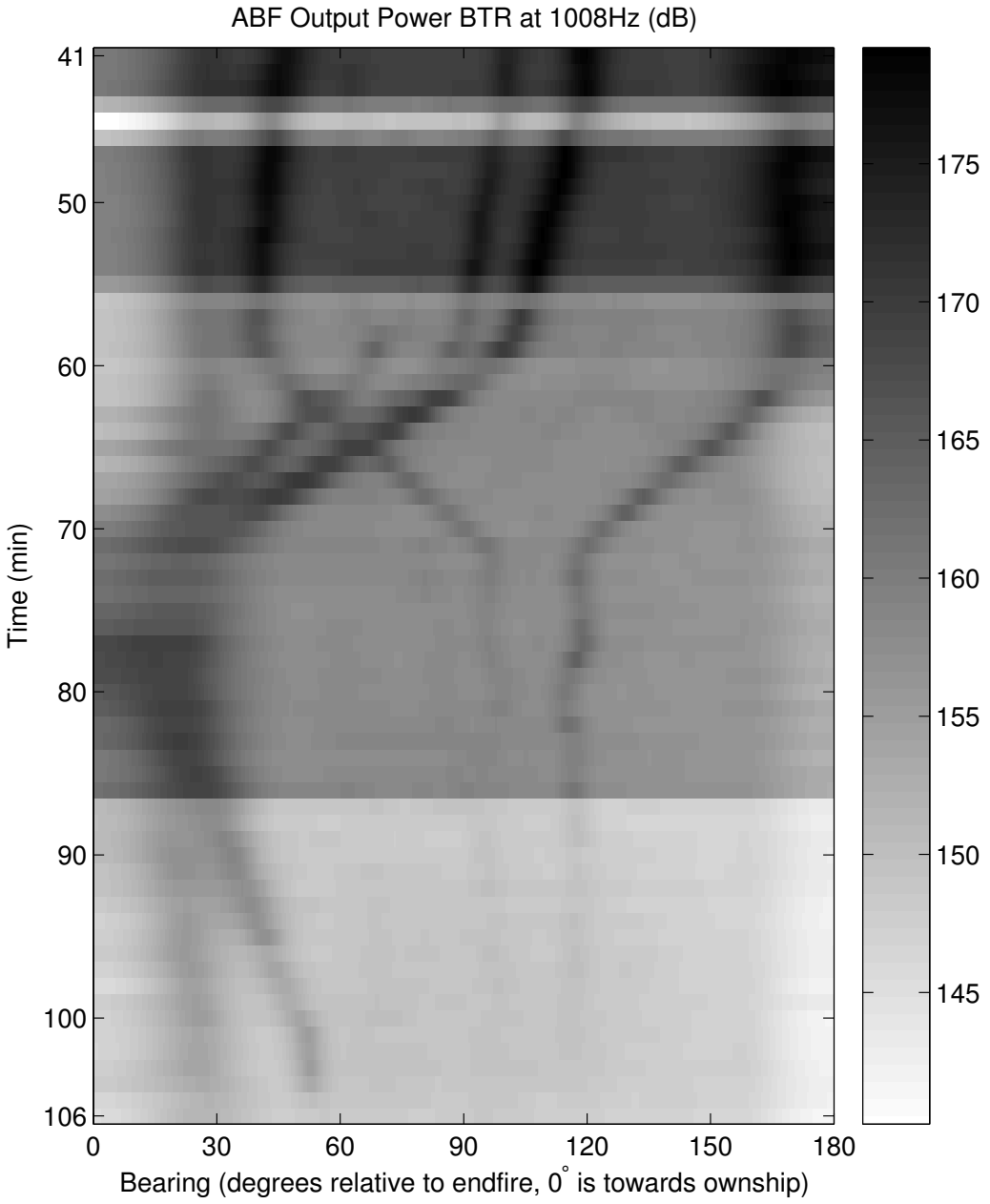

Figure 4.8: BTR showing adaptive beamformer output power. The beamformer used here is a simple, unconstrained minimum power distortionless response (MPDR) filter [48].

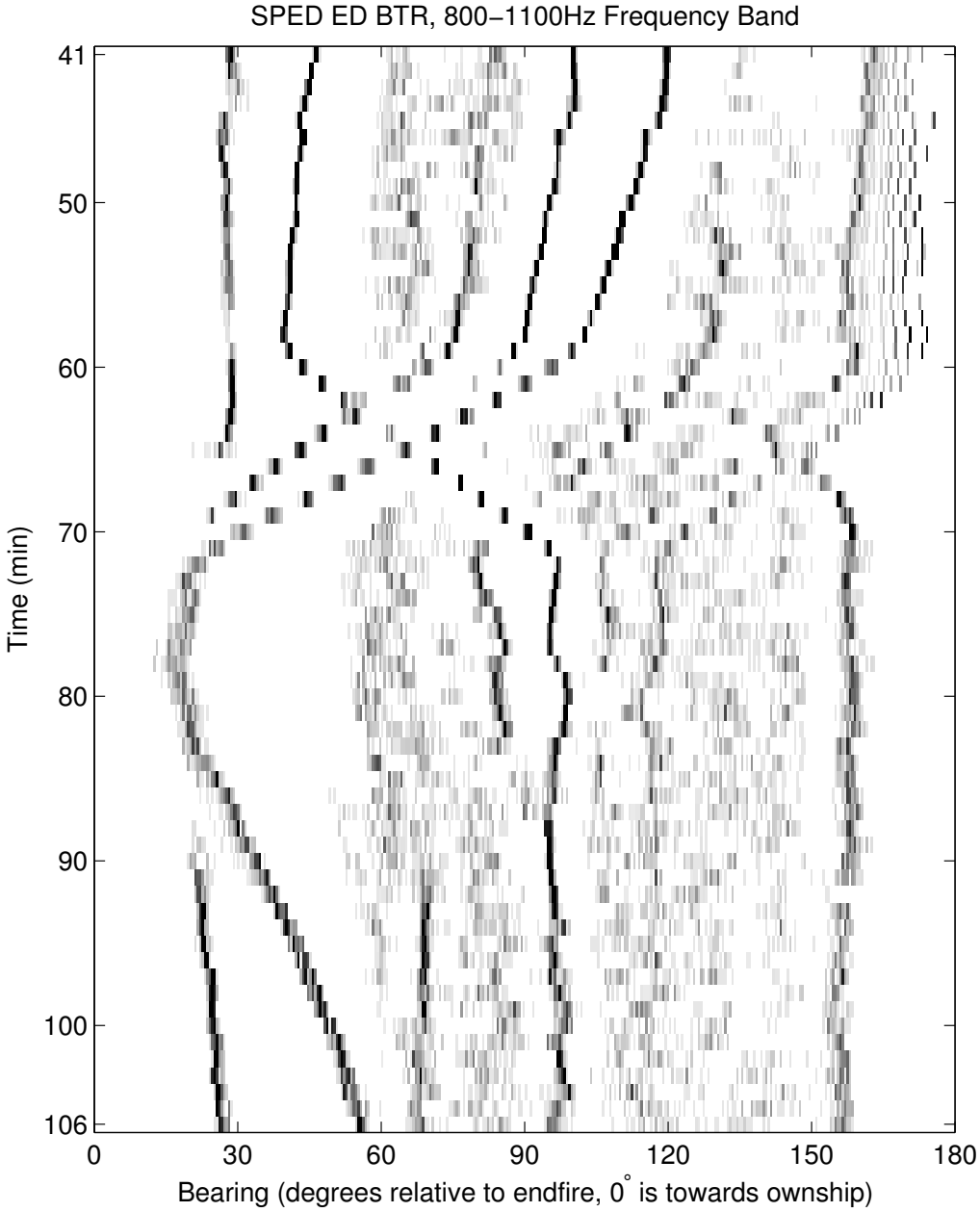

Figure 4.9: SPED ED BTR for 800-1100Hz frequency band [14]. The beamformer output power shown in Figure 4.8 was used as the input to the SPED processing.

a target-present probability of $p_1 = 0.5$.

PDFs for all interferers were generated at each measurement. The PDFs were modeled to be Gaussian with means equal to the value reported by AIS as well as equal and uncorrelated x and y variances of 1.0 km^2. This variance was assumed for the AIS tracks to account for position error from poor messaging. In addition, modeling of the Atlas array as a rigid body that follows the exact same trajectory as the Alliance, delayed in time, is an approximation that introduces some error. This is counteracted by adding additional variance to the prior PDFs of interferers.

4.2.4.2 Adding Robustness to the Signal Processing

Algorithms oftentimes perform very well when tested against ideal, simulated data. Issues of robustness frequently arise when the algorithm is tested on real-world data which may violate some of the assumptions of the underlying model. The proposed approach initially had issues of robustness in two areas when tested on data from the SEABAR 07 sea trial.

It was assumed in Section 2.1.2 that the DOA of each signal with respect to the array is constant over each scan. As a result of the large amount of time averaging in each scan (one minute), many of the signals appear to be spatially spread in bearing. This effect was mitigated by using a covariance matrix taper (CMT), originally developed independently by Mailloux and Zatman [34, 54]. The references [23, 55, 30] also provide insightful discussions on the advantages of using a CMT. For the present application, a CMT is used on all noise-plus-interference covariance matrices used during the AM algorithm of Table 4.2 and when forming

the SSLLF for the TOI; in other words,

$$\mathbf{R}_{\mathrm{n+i,t},m'} = \mathbf{R}_{\mathrm{n+i},m'} \odot \mathbf{T} \tag{4.20}$$

is used in place of $\mathbf{R}_{\mathrm{n+i},m'}$ where $\odot$ represents the Hadamard (element-wise) multiplication of two matrices, and $\mathbf{T}$ is the defined CMT. Covariance matrix tapers have the effect of null broadening in the MVDR beamformer of the SSLLF (3.9). They will also have the effect of broadening the peaks and valleys of the SSLLF terms $\beta_{m'}(\phi_{m'})$, $\alpha_{m'}(\phi_{m'})$, and $\gamma_{m'}(\phi_{m'})$. This will help to ensure that interferers that are spatially spread are properly suppressed in the SSLLF for the TOI. CMTs have been used before in the area of passive sonar, where they have been shown to increase the ability to detect weak targets that would otherwise be masked by loud moving interferers [43]. For each CMT the bearing is modeled as a Gaussian random variable with a mean equal to the MLE and a standard deviation of $\sigma = 0.01$ radians where $\mathbf{T}$ is given by [37]

$$\mathbf{T}_{pq} = \exp\left\{-\frac{1}{2}\left[d\lambda\left(p-q\right)\right]^2\sigma^2\right\} \tag{4.21}$$

and $\mathbf{T}_{pq}$ denotes the pq^{th} element of $\mathbf{T}$, where d is the inter-element spacing of the array and λ is the signal wavelength.

Another implementation issue that was experienced when analyzing the SEABAR 07 data was actually not directly related to the passive sonar signal processing but rather the implementation of the Bayesian tracker. As mentioned in Section 2.4, the PDF for the TOI is represented on a set of fixed sample points in state space where each sample point is at the center of a grid cell. The value at the sample point represents the probability over the entire grid cell. In order to obtain an accurate representation of the TOI PDF the cell spacing must be fine enough. If the likelihood function for the TOI is narrower than the cell spacing, the peaks of the

likelihood function may be missed when sampling at the center of the grid cells. The clear solution would be to increase the grid resolution, but this greatly increases the computational burden. This problem is discussed at some length in [26].

The problem predominantly exists when the ML SNR for the SOI is very large; in other words, the TOI is very loud. In order to remedy this problem it is suggested that a signal power estimate $\sigma^2_{m^\star} < \hat{\sigma}^2_{m^\star}$ be used in the SSLLF for the TOI. As discussed in Section 3.3, a smaller signal power will compress the dynamic range of the SSLLF and therefore widen the peaks. This will reduce the chance that a peak in the SSLLF be missed by the sampling of the Bayesian tracker with the trade-off of overestimating the uncertainty in the state of the TOI. This added uncertainty is quite tolerable when considering the number of approximations made in the data association and signal modeling. Care must be taken not to lower the signal power estimate too much. If it is made too small the dynamic range will be overly compressed and the SSLLF will appear flat, causing little change in the TOI state estimate. For the SEABAR 07 data set it was found that a signal power estimate that is roughly equal to the minimum detectable level (MDL) of the array, $\sigma^2_{m^\star} = \sigma^2_{\mathrm{n}}/(NK)$, worked well.

4.2.4.3 Results

Attempts to track the Leonardo were made using various model order assumptions. Either joint probabilistic data association (JPDA) or maximum association probability data association (MAP DA) and ML signal power or MDL signal power were used. The model order was varied by choosing to model subsets of the total number of potential interferers present (i.e. subsets of the list in Table 4.4). The best performance was achieved when 10 interferers were included: targets 1 through 10.

This will be referred to as the "optimal" model order. When more or less than these 10 targets were modeled there was a decrease in performance.

First, consider a scenario in which the model order is underestimated. For this scenario targets 1 through 7 were modeled as potential interferers. The results are shown in Figure 4.10. The solid lines show the AIS tracks for the Leonardo, Waterford, and Iran Amol as a reference. When the ML signal power estimate and MAP DA is used the estimated track follows the Leonardo somewhat closely up to about minute 65, when it loses it and begins to follow a track near the Waterford. The results are quite similar when the data association technique is switched to JPDA. Next, consider the case when the MDL is used for the signal power estimate. This scenario performs much better, with both MAP DA and JPDA having very little estimation error. JPDA outperforms MAP DA from approximately minute 41 to 47. In all cases the track on the Leonardo is somewhat lost after about minute 90. This is roughly the time the Leonardo makes its second sharp maneuver. Based on these results it appears that the use of the MDL for the signal power estimate and JPDA provide the best performance and robustness.

Another important regime to discuss occurs between about minute 41 and minute 50. In this area there are sharp jumps in the estimated bearing. Due to the inherent left-right ambiguity of a linear array, the Bayesian tracker places an equal amount of probability mass on each side of the array. This results in the MAP estimate of the TOI PDF jumping between sides of the array. The ambiguity is resolved some time after minute 50 because the Alliance (which is towing the Atlas array) makes a maneuver. As can be seen in Figure 4.7 this maneuver allows the range from the Alliance to the Leonardo to be somewhat localized. This localization happens quite naturally in a Bayesian framework whereas significant work needs to

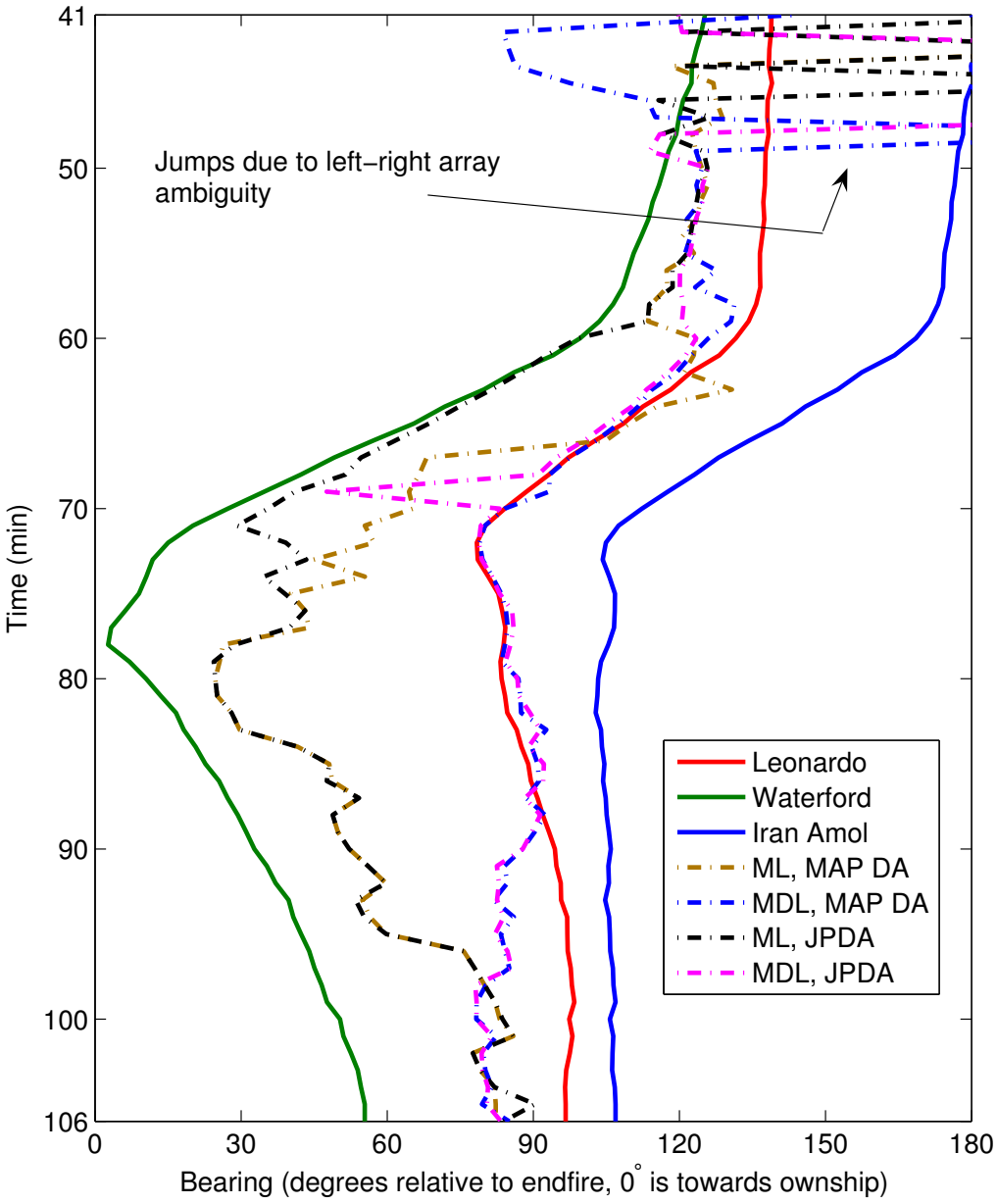

Figure 4.10: Estimated BTRs, results for underestimated model order.

be done to linearize measurements when using a standard Kalman type filter [29].

Now, consider a scenario in which the model order is overestimated. This is an interesting scenario because one might imagine that by overestimating the model order the joint LF could be sub-optimally marginalized at the expense of increased computational demand. In other words, one would hope that if the TOI were detectable it would be represented by at least one of the marginal LFs. The difficulty in this case is association of the correct marginal LF with the TOI. For this scenario targets 1 through 10 and 14 and 15 were modeled as potential interferers. Only the use of the MDL for the signal power estimate and JPDA were considered as they appear to be the most robust choices. The results for this scenario are shown in Figure 4.11. This scenario has a significantly smaller estimation error from minute 41 to 60. It also does not have the spike in estimation error at minute 69 that the underestimated model order does. Unfortunately, similar to the underestimated model order, the overestimated model order somewhat loses the track of the Leonardo at about the time it makes its second sharp maneuver (minute 90). Based on these results it would appear it is better to overestimate the model order rather than underestimate, the cost being an increased computational demand for the higher model order.

Finally, consider the scenario in which the model order of best performance, or the "optimal" model order, is chosen, the MDL is used for the signal power estimate, and JPDA is performed. The results for this scenario are shown in Figure 4.11. The estimation error for this scenario is quite low. The most important thing to note is that the track is maintained after the Leonardo makes its second sharp maneuver. This scenario does have a slight increase in estimation error between about minute 70 and 80 in comparison to the other scenarios.

An interesting variation of the above scenario, also shown in Figure 4.11, is the

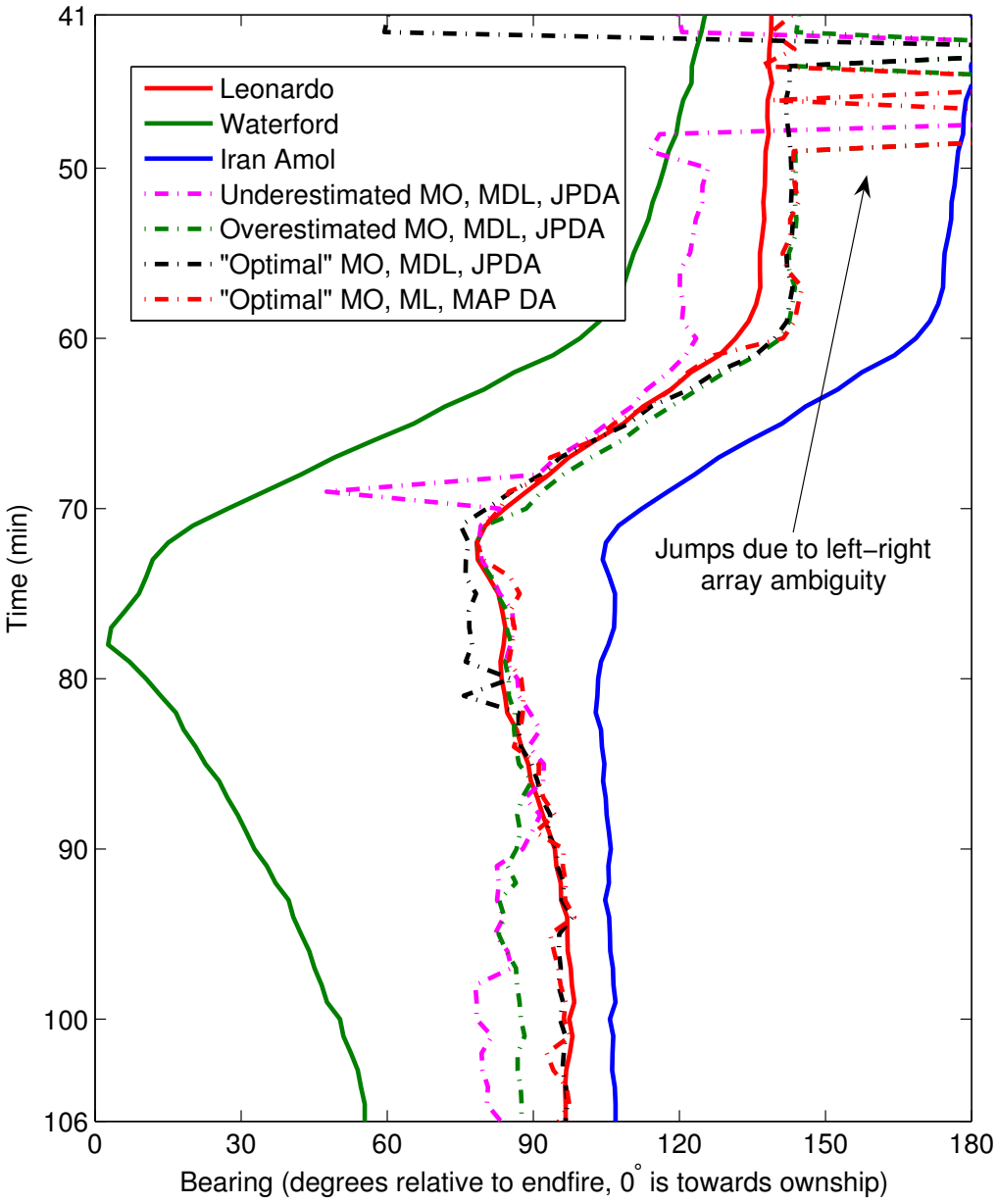

Figure 4.11: Estimated BTRs, results for various model orders.

one in which the "optimal" model order is again used, but now the MLE is used for the signal power and MAP DA is performed. This scenario performs better than any of the others presented, and, in fact, performs better than the many other scenarios investigated by the author but not shown in this thesis. The scenario performs very similar to the MDL/JPDA scenario, but it has decreased estimation error between minute 70 and 80. Although this scenario performs the best, it was shown earlier that the use of the MDL for the signal power estimate and JPDA were the most robust when the "optimal" model order is not chosen. In practice, the use of MDL/JPDA should be preferred in order to provide robustness against mismatched model order.

One final remark regarding the analysis of the SEABAR 07 data set is that during the sea trial there may have been other vessels present for which there was no AIS information available. This would help to explain many of the lost tracks in Figure 4.10 and Figure 4.11. For example, the lost track that follows the second sharp maneuver of the Leonardo does not correspond to any of the 30 known AIS tracks. This could indicate unexplained error in the signal processing, but it more likely corresponds to an unknown target in the area.

Chapter 5

Conclusions and Future Work

Bayesian tracking of the DOA of a single target of interest (TOI) in the presence of potential interferers was presented. Statistical models and a background of beamforming were also discussed. It was shown that when noise and interferer parameters are known the likelihood function for a single-signal is a function of the output of the popular minimum variance distortionless response (MVDR) beamformer. Marginalization of the joint likelihood function for all signals was achieved by using maximum likelihood estimates (MLEs) in the place of nuisance parameters. This approach was shown to be very successful in suppressing the influence of interferers in the single-signal likelihood function, even when there was much a priori uncertainty in the interferer locations.

Prior information regarding the location of the TOI and potentially interfering targets was utilized to increase performance in terms of improved detection and decreased estimation error. This had the added benefit of increasing computational efficiency. The scenario of an unknown number of interfering targets was investigated in Section 4.2. It was demonstrated that when the correct number of interfering targets is modeled a quiet TOI can be tracked in an environment cluttered with many interferers. This was achieved by performing data association between the signal MLEs and the TOI. Association probabilities were calculated using a computationally efficient approximate formula that includes a heuristic expression which censors

data from potentially interfering targets.

When the number of interfering targets is known a priori the need to perform data association can be circumvented by utilizing available prior information. This was achieved by using the proposed approaches of cued beamforming and the feedback of signal MLEs. Although the proposed approach did not guarantee that the produced MLEs were true MLEs, it was able to obtain comparable or improved performance in comparison to a conventional approach that uses no prior information.

There is a significant amount of future work related to this topic. Perhaps the most apparent is the unification of the approaches of Section 4.1 and Section 4.2. That is, it would be desirable to combine the approaches if there were some targets that produced definite interfering signals and some that produced only potentially interfering signals. This would closely be related to investigating the scenario in which the number of modeled signals is not equal to the number of modeled targets ($M \neq L$). One could also modify the algorithms presented to allow the signal model order to vary each scan based on a user-defined SNR threshold for MLEs.

Additional future work could involve the development of an improved expression for calculating the association probabilities. Most importantly, the heuristic expression defined in (4.12) could be replaced with a more principled expression that is a function of the probability of resolution.

Finally, results could be extended to the tracking of multiple targets of interest and fusion with active sonar. The SEABAR 07 data set is a strong candidate for active-passive data fusion as active sonar was operating at the same time as the run analyzed in this thesis. It would be interesting to investigate whether the information provided by active sonar would be enough to disambiguate the TOI signal from the interfering targets' signals.

Appendix A

Approximation of the Association Likelihood Function

As discussed in Section 4.2.2.2 the summation in (4.10) is computationally infeasible because the summation over possible associations, i, must consider all possible permutations of signal to target associations. When associating the M signal DOA MLEs with the M currently tracked targets it is assumed that each signal m can only have originated from one target l. In this case each association i is a permutation of $\{1, 2, ..., M\}$ where there are no repeated entries. In equation (4.10) $i_1 = m$, or in other words the MLE with index m is assumed to be associated with target $l = 1$. Since one component in i is fixed there are a total of $(M-1)!$ different associations and therefore $(M-1)!$ terms to sum over.

Suppose now that the constraint that each signal m can only have originated from one target l is relaxed. This means that each association i can now be any combination of $\{1, 2, ..., M\}$, where now repeated entries are allowed. Note again that $i_1 = m$ is enforced. There are now a total of $(M-1)^{M-1}$ possible associations. A straightforward computation of (4.10) thus requires a summation over $(M-1)^{M-1}$ terms which is much more computationally complex than before. Luckily, this computation can be greatly reduced by factoring.

Consider the case where $M = 3$ and $m = 1$. In this case the possible associations are $i = (1, 2, 2)$, $(1, 2, 3)$, $(1, 3, 2)$, and $(1, 3, 3)$. The right hand side of (4.10)

can thus be expanded as

$$\sum_{i:i_1=1}\prod_{l=2}^{3}\rho_l\left(\hat{\phi}_{i_l}\right)=\rho_2\left(\hat{\phi}_2\right)\rho_3\left(\hat{\phi}_2\right)+\rho_2\left(\hat{\phi}_2\right)\rho_3\left(\hat{\phi}_3\right)$$
$$+\rho_2\left(\hat{\phi}_3\right)\rho_3\left(\hat{\phi}_2\right)+\rho_2\left(\hat{\phi}_3\right)\rho_3\left(\hat{\phi}_3\right). \quad \text{(A.1)}$$

This expression contains the extra terms $\rho_2\left(\hat{\phi}_2\right)\rho_3\left(\hat{\phi}_2\right)$ and $\rho_2\left(\hat{\phi}_3\right)\rho_3\left(\hat{\phi}_3\right)$ that would not normally be found in the more exact expression (4.10). If targets are widely spaced then it is unlikely that two prior PDFs will both have a value much greater than zero at the same DOA. Since one of the factors in each of the extra terms will be close to zero the total term will also be close to zero. Relaxing the constraint that each signal m can only have originated from one target l is therefore a good approximation when targets are widely spaced. The expression (A.1) can be factored as

$$\sum_{i:i_1=1}\prod_{l=2}^{3}\rho_l\left(\hat{\phi}_{i_l}\right)=\left(\rho_2\left(\hat{\phi}_2\right)+\rho_2\left(\hat{\phi}_3\right)\right)\times\left(\rho_3\left(\hat{\phi}_2\right)+\rho_3\left(\hat{\phi}_3\right)\right). \quad \text{(A.2)}$$

By generalizing to arbitrary M and m the following equality is obtained:

$$\sum_{i:i_1=m}\prod_{l=2}^{M}\rho_l\left(\hat{\phi}_{i_l}\right)=\prod_{l=2}^{M}\sum_{\substack{j=1\\ j\neq m}}^{M}\rho_l\left(\hat{\phi}_j\right). \quad \text{(A.3)}$$

Equation (4.10) can therefore be approximated as (4.11). The expression (A.3) contains the sum of $(M-1)^2$ terms and the product of $M-1$ factors. The computational complexity of computing (4.11) is therefore much less than computing (4.10). Note that, although this approximation relaxes the one signal to one target association constraint on some targets, it does not relax the constraint on the signal m to target $l=1$ association. That is, signal m may not be associated with any target $l\neq 1$, and no signal besides signal m may be associated with target $l=1$.

Bibliography

[1] A. Amar and A. Weiss, "Fundamental limitations on the number of resolvable emitters using a geolocation system," *IEEE Trans. Signal Process.*, vol. 55, no. 5, pp. 2193–2202, May 2007.

[2] J. M. Aughenbaugh and B. R. La Cour, "Use of prior information in active sonar tracking," in *Proc. 12th Int. Conf. on Information Fusion*, Seattle, WA, Jul. 2009.

[3] A. Baggeroer and H. Cox, "Passive sonar limits upon nulling multiple moving ships with large aperture arrays," in *Conference Record of the Thirty-Third Asilomar Conference on Signals, Systems, and Computers*, vol. 1, Oct. 1999, pp. 103–108.

[4] Y. Bar-Shalom, *Tracking and Data Association*. Boston, MA: Academic Press, 1988.

[5] Y. Bar-Shalom and X.-R. Li, *Multitarget-Multisensor Tracking: Principles and Techniques*. Storrs, CT: YBS Publishing, 1995.

[6] K. L. Bell, Y. Ephraim, and H. L. Van Trees, "A Bayesian approach to robust adaptive beamforming," *IEEE Trans. Signal Process.*, vol. 48, no. 2, pp. 386–398, Feb. 2000.

[7] K. L. Bell and R. Pitre, "MAP-PF 3D position tracking using multiple sensor array," in *Proc. 5th IEEE Sensor Array and Multichannel Signal Process. Workshop*, Jul. 2008, pp. 238–242.

[8] R. E. Bethel, "Joint detection and estimation in a multiple signal array processing environment." Ph.D. dissertation, George Mason University, Fairfax, VA, Aug. 2002, available at (http://gunston.gmu.edu/kbell/pubs/BethelDissert.pdf).

[9] ——, "MLE derivations and performance demonstrations for narrowband detection and estimation," George Mason University, Fairfax, VA, Tech. Rep., Nov. 2003, available at (http://gunston.gmu.edu/kbell/pubs/BethelDetEst.pdf).

[10] R. E. Bethel and K. L. Bell, "A MLE approach to joint array detection and direction of arrival estimation," in *Proc. Sensor Array and Multichannel Signal Processing Workshop*, Aug. 2002, pp. 169–173.

[11] R. E. Bethel and G. J. Paras, "A PDF multisensor multitarget tracker," *IEEE Trans. Aerosp. Electron. Syst.*, vol. 34, no. 1, pp. 153–168, Jan. 1998.

[12] R. Bethel and K. Bell, "A correlated signals mle approach to joint source detection and direction of arrival estimation," in *Proc. IEEE Workshop on Statistical Signal Processing*, Sep. 2003, pp. 446–449.

[13] ——, "Maximum likelihood approach to joint array detection/estimation," *IEEE Trans. Aerosp. Electron. Syst.*, vol. 40, no. 3, pp. 1060–1072, July 2004.

[14] M. Bono, R. Bethel, P. McCarty, and B. Shapo, "Subband energy detection methods in passive array processing," in *Proc. MIT Lincoln Laboratory Adaptive Sensor Array Processing (ASAP) Workshop*, Mar. 2001.

[15] J. Capon, "High-resolution frequency-wavenumber spectrum analysis," *Proc. IEEE*, vol. 57, no. 8, pp. 1408–1418, Aug. 1969.

[16] H. Cox, R. Zeskind, and M. Owen, "Robust adaptive beamforming," *IEEE Trans. Acoust., Speech, Signal Process.*, vol. 35, no. 10, pp. 1365–1376, Oct. 1987.

[17] H. Cox, "Resolving power and sensitivity to mismatch of optimum array processors," *J. Acoust. Soc. Am.*, vol. 54, no. 3, pp. 771–785, Sep. 1973.

[18] F. Ehlers, "Final report on deployable multistatic sonar systems," Tech. Rep. NURC-FR-2009-001, Jan. 2009, NATO UNCLASSIFIED.

[19] M. Feder and E. Weinstein, "Parameter estimation of superimposed signals using the EM algorithm," *IEEE Trans. Acoust., Speech, Signal Process.*, vol. 36, no. 4, pp. 477–489, Apr. 1988.

[20] R. P. Goddard, "The sonar simulation toolset," in *Proc. OCEANS*, vol. 4, Sep. 1989, pp. 1217–1222.

[21] ——, "The Sonar Simulation Toolset, Release 4.1: Science, Mathematics, and Algorithms," Applied Physics Laboratory, University of Washington, Seattle, Tech. Rep. APL-UW 0404, Oct. 2002.

[22] N. J. Gordon, D. J. Salmond, and A. F. M. Smith, "Novel approach to nonlinear / non-gaussian bayesian state estimation," *IEE Proceedings F Radar and Signal Processing*, vol. 140, no. 2, pp. 107–113, Apr. 1993.

[23] J. Guerci, "Theory and application of covariance matrix tapers for robust adaptive beamforming," *IEEE Trans. Signal Process.*, vol. 47, no. 4, pp. 977–985, Apr. 1999.

[24] D. Hall and J. Llinas, "An introduction to multisensor data fusion," *Proc. IEEE*, vol. 85, no. 1, pp. 6–23, Jan. 1997.

[25] R. E. Kalman, "A new approach to linear filtering and prediction problems," *Transactions of the ASME – Journal of Basic Engineering*, vol. 82 (Series D), pp. 35 – 45, 1960.

[26] C. M. Kreucher, B. Shapo, and R. Bethel, "Multitarget detection and tracking using multi-sensor passive acoustic data," in *Proc. IEEE Aerospace conference*, 2009, pp. 1–16.

[27] B. R. La Cour, "Ensemble-based Bayesian detection and tracking," in *Proc. Meetings Acoust.*, vol. 1, 055001, Feb. 2008.

[28] ——, "Stationary priors for Bayesian target tracking," in *Proc. Int. Conf. on Information Fusion*, Cologne, Germany, Jul. 2008.

[29] B. La Scala and M. Morelande, "An analysis of the single sensor bearings-only tracking problem," in *Proc. 11th Int. Conf. on Information Fusion*, Cologne, Germany, 2008, pp. 1–6.

[30] J. Li, P. Stoica, and T. Yardibi, "Covariance beamforming, covariance matrix tapers and matrix beamforming are related," *Electronics Letters*, vol. 44, no. 5, pp. 383–384, Feb. 2008.

[31] J. Li and P. Stoica, *Robust Adaptive Beamforming*. Hoboken, New Jersey: Wiley Series in Telecommunications and Signal Processing, 2006.

[32] R. G. Lyons, *Understanding Digital Signal Processing, Second Edition*. Upper Saddle River, NJ: Prentice Hall, 2004.

[33] C. MacInnes, "Source localization using subspace estimation and spatial filtering," *IEEE J. Ocean. Eng.*, vol. 29, no. 2, pp. 488–497, Apr. 2004.

[34] R. Mailloux, "Covariance matrix augmentation to produce adaptive array pattern troughs," *Electronics Letters*, vol. 31, no. 10, pp. 771–772, May 1995.

[35] M. M. Morelande, "Joint data association using importance sampling," in *Proc. 12th Int. Conf. on Information Fusion*, Seattle, WA, Jul. 2009.

[36] B. Ottersten, M. Viberg, P. Stoica, and A. Nehorai, "Exact and Large Sample ML Techniques for Parameter Estimation and Detection in Array Processing," in *Radar Array Processing*, S. Haykin, J. Litva, and T. J. Sheperd, Eds. Berlin: Springer-Verlag, 1993.

[37] J. Riba, J. Goldberg, and G. Vazquez, "Robust beamforming for interference rejection in mobile communications," *IEEE Trans. Signal Process.*, vol. 45, no. 1, pp. 271–275, Jan. 1997.

[38] C. Richmond, "Capon algorithm mean-squared error threshold SNR prediction and probability of resolution," *IEEE Trans. Signal Process.*, vol. 53, no. 8, pp. 2748–2764, Aug. 2005.

[39] B. D. Ripley, *Stochastic Simulation*. New York: Wiley Series in Probability and Mathematical Statistics, 1987.

[40] R. Roy and T. Kailath, "ESPRIT – estimation of signal parameters via rotational invariance techniques," *IEEE Trans. Acoust., Speech, Signal Process.*, vol. 37, no. 7, pp. 984–995, Jul. 1989.

[41] R. Schmidt, "Multiple emitter location and signal parameter estimation," *IEEE Trans. Antennas Propag.*, vol. 34, no. 3, pp. 276–280, Mar. 1986.

[42] B. Shapo and R. Bethel, "An overview of the probability density function (PDF) tracker," in *Proc. OCEANS 2006*, Sep. 2006, pp. 1–6.

[43] H. Song, W. Kuperman, W. Hodgkiss, P. Gerstoft, and J. S. Kim, "Null broadening with snapshot-deficient covariance matrices in passive sonar," *IEEE J. Ocean. Eng.*, vol. 28, no. 2, pp. 250–261, Apr. 2003.

[44] S. Stergiopoulos, "Implementation of adaptive and synthetic-aperture processing schemes in integrated active-passive sonar systems," *Proc. IEEE*, vol. 86, no. 2, pp. 358–398, Feb. 1998.

[45] L. D. Stone, T. L. Corwin, and C. A. Barlowe, *Bayesian Multiple Target Tracking*. Boston, MA: Artech House, 1999.

[46] L. D. Stone, T. L. Corwin, and J. B. Hofmann, "Technical documentation of Nodestar," Naval Research Laboratory Technical Report, Tech. Rep. NRL/FR/5580–95-9788, 1995.

[47] United States Coast Guard Navigation Center, "Automatic identification system overview," (http://www.navcen.uscg.gov/enav/AIS/default.htm), Retrieved February 12, 2009.

[48] H. L. Van Trees, *Detection, Estimation, and Modulation Theory, Part IV, Optimum Array Processing*. New York: Wiley, 2002.

[49] M. Wax and I. Ziskind, "On unique localization of multiple sources by passive sensor arrays," *IEEE Trans. Acoust., Speech, Signal Process.*, vol. 37, no. 7, pp. 996–1000, Jul. 1989.

[50] B. A. Yocom, T. W. Yudichak, and B. R. La Cour, "Passive beamforming enhancements in relation to active-passive data fusion," in *Proc. IEEE Asilomar Conf. on Signals, Systems, and Computers*, Pacific Grove, CA, Oct. 2008.

[51] ——, "Bayesian passive sonar tracking in the presence of known interferers," in *Proc. 12th Int. Conf. on Information Fusion*, Seattle, WA, Jul. 2009.

[52] T. W. Yudichak, B. A. Yocom, and M. Le, "Cued beamforming of passive arrays in the context of active-passive data fusion," in *Acoust. Soc. Am. Proc. of Meetings on Acoust.*, vol. 2, Jun. 2008, pp. 1–8.

[53] ——, "Cued passive bearing estimation in distributed sensor data fusion," in *Proc. 11th Int. Conf. on Information Fusion*, Cologne, Germany, Jul. 2008.

[54] M. Zatman, "Production of adaptive array troughs by dispersion synthesis," *Electronics Letters*, vol. 31, no. 25, pp. 2141–2142, Dec. 1995.

[55] M. Zatman and J. Guerci, "Comments on 'Theory and application of covariance matrix tapers for robust adaptive beamforming' [and reply]," *IEEE Trans. Signal Process.*, vol. 48, no. 6, pp. 1796–1800, Jun. 2000.

[56] I. Ziskind and M. Wax, "Maximum likelihood localization of multiple sources by alternating projection," *IEEE Trans. Acoust., Speech, Signal Process.*, vol. 36, no. 10, pp. 1553–1560, Oct. 1988.

Vita

Bryan Alan Yocom was born on May 11, 1984 in Joliet, IL. He was raised in Lockport, IL where he achieved the rank of Eagle Scout through the Boy Scouts of America. After high school he attended the University of Illinois, Urbana-Champaign. In May 2007 he graduated with honors with the B.S. degree in electrical engineering. Bryan was also a member of Eta Kappa Nu and Phi Kappa Phi honor societies while at the University of Illinois.

Since August 2007, he has been a graduate research assistant at Applied Research Laboratories, The University of Texas, Austin. He is currently specializing in acoustics and digital signal processing with research interests in array signal processing, data-fusion, and statistical signal processing for sonar applications. He is also a student member of the Institute of Electrical and Electronics Engineers (IEEE).

Permanent address: 3301 Speedway Apt. 105
Austin, Texas 78705

This thesis was typeset with LaTeX[†] by the author.

[†]LaTeX is a document preparation system developed by Leslie Lamport as a special version of Donald Knuth's TeX Program.